MURDOCH UNIVERSITY SCHOOL OF ENGINEERING AND INFORMATION TECHNOLOGY

Modelling and Simulating a Three-Phase Induction Motor

ENG460 Engineering Thesis

Benjamin Willoughby

3/3/2014

Executive Summary

This project involves modelling and simulating a real three-phase induction motor to determine its transient and steady-state characteristics, such as its torque-speed characteristics, torque-time characteristics, speed-time characteristics and its rotor and stator currents. For the simulation the computer program MATLAB/Simulink was used. The motors equivalent circuit parameters were determined by performing the standard equivalent circuit parameter tests; the DC test, no-load test and the blocked-rotor test. The moment of inertia of the motor was attempted to be determined through power and deceleration tests, although the method proposed in this paper proved to be unsuccessful. The resulting equivalent circuit parameters determined from the suggested tests were highly unlikely for the 0.37 kW motor used, however the MATLAB/Simulink computer program proved to be a suitable program to simulate three-phase induction motors.

Acknowledgements

Table of Contents

1 Introduction

Three-phase induction motors are the most common type of motor used for industrial applications because of their simplicity, rugged construction and low cost (Ned Mohan, 2003; Hambley, 2008). It is important to understand their steady-state as well as their transient characteristics. It is not always possible or feasible to measure all of these characteristics; therefore, it is advantageous to build a mathematical model of the motor in order to simulate its performance. The computer program MATLAB/Simulink is an appropriate tool for such simulations.

The main objective for this project is to model and simulate a real three-phase induction motor in order to understand its steady-state and transient characteristics such as its torque-speed characteristics, torque-time characteristics, speed-time characteristics and rotor and stator currents, most of which are extremely difficult to measure.

In order to develop such a simulation the motors equivalent circuit parameters must be known; these include the motor's stator and rotor resistances and inductances as well as the magnetising reactance. These parameters are determined by performing a DC test, no-load test and blocked-rotor test on the motor. The motor's moment of inertia also must be known in order to obtain accurate dynamic simulations.

The equations that determine a three-phase induction motor's performance are extremely complicated, due to time varying inductances; therefore it is advantageous to implement a change of reference frames, commonly known as the Park's transformation. The Park's transformation implements a transformation from the conventional abc reference frame to a dq0 reference frame, which eliminates the time dependant inductances in the equations. This greatly simplifies the analysis. Therefore, in this thesis a dq0 reference frame is adapted.

2 Literature Review

2.1 Introduction

The literature review provides the background to this project. It begins with the three-phase induction motor, outlining the theory of its operation including its construction and how torque is generated. The next part outlines the equivalent circuit of the induction motor and the relevant equations needed to understand and simulate its performance. This part also covers the experiments that need to be performed on an induction motor in order to acquire the motors equivalent circuit parameters. These tests include the no-load test, the blocked-rotor test, the DC test and methods to calculate the motor's moment of inertia. The penultimate section of this chapter discusses in great depth the reference frame theory for electrical machines, outlining relevant transformations of reference frames before discussing the equations associated with modelling a three-phase induction motor. The final section of this chapter outlines the simulation of induction machines comparing different simulations as well simulations in different frames of reference.

2.2 Three-Phase Induction Motor

2.2.1 Construction

A three-phase induction motor consists of two main components, a stator and a rotor. The stator is the outside component and remains fixed, while the rotor sits inside the stator, separated by a small air gap, and, as its name suggests, it rotates, delivering the required mechanical energy.

The stator consists of a laminated iron core with many uniformly set slots running vertically throughout. The slots are wound with copper wire to create the coils needed to induce a rotating magnetic field (RMF) from a three-phase power supply (Hambley, 2008).

There are two types of rotors used in induction motors, the wound rotor and the squirrel cage rotor. The squirrel type rotor is made out of a laminated iron core with many uniform slots; however, these slots consist of aluminium bars instead of copper coils. The rotor also has two rings on each end to short circuit the bars (Chapman, 2012). The reason for this is outlined below. The other type of rotor is the wound rotor; instead of having aluminium

bars through the slots in its core, it consists of copper windings, much like in the stator. These winding are connected to three slip rings, one for each phase, which are contacted by brushes. The brushes are connected to varying resistances to control the starting current of the machine and are used also for speed control (Chapman, 2012). The squirrel cage rotor is the most common type of rotor, this is because it has a much less complex design; it does not require slip rings or brushes and, therefore, is less expensive and requires less maintenance (Chapman, 2012).

Three-phase induction motors also consist of a sturdy metal frame to hold the stator in place and reduce vibrations, and a fan connected to the rotor to cool the machine during operation.

2.2.2 Principal of Operation

When a three-phase balanced alternating current, separated by 120 degrees per phase, flows into each of the three-phase stator windings, a rotating magnetic field, or rotating magnetic flux (RMF), is produced through the stator core. The speed of RMF is called the synchronous speed. The synchronous speed if the motor is determined by the frequency of the supply and the number of poles in the motor (Chapman, 2012; Hambley, 2008). Synchronous speed is defined by:

$$n_s = \frac{120 * f}{p} \quad (1)$$

where; n_s is the synchronous speed in revolutions per minute (revs/min), f is the frequency (Hertz), and p represents the number of poles in the machine.

The RMF that is generated through the stator windings produces a magnetic field that rotates throughout the air gap. This magnetic field cuts through the short-circuited rotor bars, inducing a voltage; this voltage causes a current to flow through the rotor bars, which in turn induces a magnetic field through the rotor. This resulting magnetic field interacts with the stator magnetic field generating a force which drives the motor. The torque produced by a magnetic field is proportional to the flux density and the rotor current.

The rotor will never rotate at synchronous speed, because this will result in the stator magnetic field not being able to cut through the rotor bars to induce a voltage. So the rotor will always rotate at a slower speed to the stator magnetic field (Keljik, 2009) .

The difference in the rotor speed and the synchronous speed is known as the slip. The slip is essentially caused by any torque acting against the rotor of the motor slowing it down below the synchronous speed. Slip speed can be represented by the following equation:

$$n_{slip} = n_s - n_r = \omega_s - \omega_r \quad (2)$$

Where n_{slip} represents the slip speed, n_s and ω_s represent the synchronous speed in revs/min, and n_r and ω_r represent the mechanical speed of the rotor.

The slip is defined as the relative mechanical speed as a fraction of synchronous speed. Such that:

$$s = \frac{n_s - n_r}{n_s} = \frac{\omega_s - \omega_r}{\omega_s} \quad (3)$$

where s = slip, n =speed (revs/min), ω = angular velocity (radians per second) and the subscripts s and r represent the synchronous speed and the speed of the rotor respectively.

From this definition it can be seen that when slip is equal to zero, the motor is operating at synchronous speed, and when the slip is 1, the rotor is locked.

Using this definition of slip, the rotor frequency is given by:

$$f_{re} = s f_{se} \quad (4)$$

where f_{se} refers to the system frequency in hertz.

Incorporating the synchronous speed equation:

$$f_{re} = \frac{P}{120}(n_s - n_m)$$

where n_m refers to the speed of the motor in revs/min.

(5)

The equivalent circuit of an induction motor is a useful tool in analysing its performance; it can be used to derive the power and torque equations relating to the operation of the motor. The per phase equivalent circuit of an induction motor is shown in the figure below.

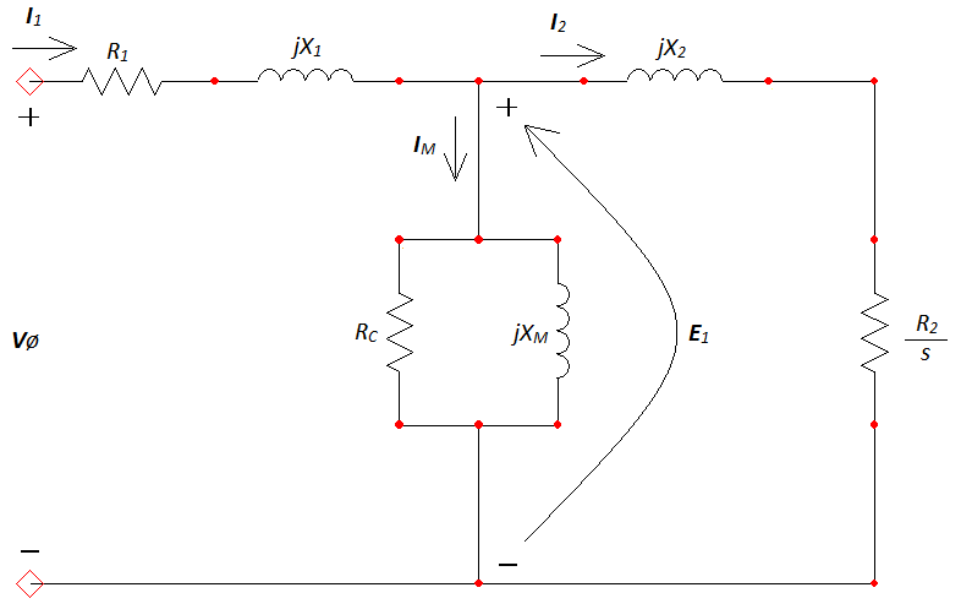

Figure 1: Per-phase equivalent circuit of an induction motor

Referring to figure 1; I_1 represents the stator current in amps, V_ϕ represents the per phase voltage in volts, R_1 and X_1 represent the stator's resistance and impedance respectively in ohms, I_M represents the magnetising current in amps, R_C represents the core resistance in ohms, X_M represents the magnetising inductance in ohms, E_1 refers to the induced voltage on the rotor in volts, I_2 represents the rotor current in amps, X_2 and R_2 refer to the rotor impedance and resistance respectively in ohms.

From the above figure, the per phase input current can be calculated by:

$$\mathbf{I}_1 = \frac{\mathbf{V}_\phi}{Z_{eq}} \qquad (6)$$

The electrical input power of an induction motor P_{in} can be found from the phase voltage, line current and the power factor; it is described by the equation:

$$P_{in} = 3V_{\phi}\, I_1\, cos\theta \quad (7)$$

There are many power losses that occur within an induction motor, from the electrical input power to the mechanical output power that is developed. The first of these losses occur within the stator copper windings, these are called the stator copper losses P_{SCL} and are given by the equation:

$$P_{SCL} = 3I^2{}_1 R_1 \quad (8)$$

Eddy currents and hysteresis that occur within the stator windings also account for power losses; these are called core losses P_{core} and are derived by the equation:

$$P_{core} = 3E^2{}_1 R_C \quad (9)$$

The remaining power is then transferred across the air gap to the rotor. This is called the air-gap power P_{AG}. From the equivalent circuit it can be seen that the only element that can consume the air-gap power is the rotor resistor R_2/s. Therefore the air-gap power is derived by the equation:

$$P_{AG} = P_{in} - P_{SCL} - P_{core} = 3I^2{}_2 \frac{R_2}{s} \quad (10)$$

The last of the electrical power losses occur within the rotor, much like the stator copper losses these are called rotor copper losses P_{RCL}, although not all rotors consist of copper windings. P_{RCL} is derived from the equation:

$$P_{RCL} = 3I^2{}_2 R_2 \quad (11)$$

The power that remains is what is converted from electrical power to mechanical power. This converted power P_{conv} is derived from the equation:

$$P_{conv} = P_{AG} - P_{RCL} = 3I^2{}_2 R_2 \left(\frac{1-s}{s}\right) = (1-s)P_{AG} \quad (12)$$

The final losses that occur within an induction motor are the friction and windage losses. These account for the inertia of the rotor and the fan and the friction between the rotor and the bearings. These losses are called rotational losses P_{rot}. If the rotational losses are known, the output power P_{out} can be found by:

$$P_{out} = P_{conv} - P_{rot} \quad (13)$$

The output power can also be calculated from the load torque and the speed of the rotor.

$$P_{out} = \tau_{load}\omega_m \quad (14)$$

The load torque τ_{load} of the machine can be found from the equation:

$$\tau_{ind} = \frac{P_{conv}}{\omega_m} = \frac{P_{AG}}{\omega_s} \quad (15)$$

The torque produced by a three-phase induction motor primarily depends on the mutual inductance, the current and the slip (Puri).

Where the induced torque on the load τ_{load} can be found from:

$$\tau_{load} = \frac{P_{out}}{\omega_m} \quad (16)$$

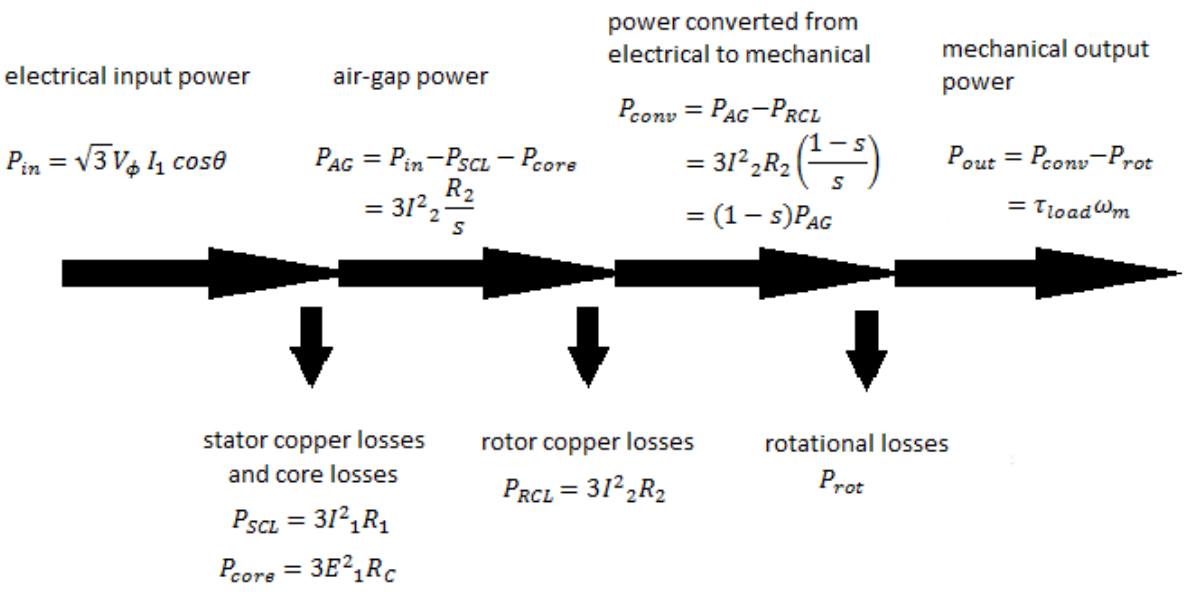

Figure 2: Power flow diagram of an induction motor

The stator self-inductances are all equal, as shown in figure 17.

$$L_{asas} = L_{bsbs} = L_{cscs} \quad (17)$$

Where: $L_{asas} = L_{ls} + L_{ms}$

The magnetising inductance L_{ms} is calculated from the equation:

$$L_{ms} = \left(\frac{N_s}{2}\right)^2 \frac{\pi\mu_0 rl}{g} \quad (18)$$

The voltage equations for a three-phase induction motor are derived from the supplied current and the internal resistances, as in normal voltage equations, although they are also dependant on the magnetic flux linkages with respect to time, which makes the equations very complex. The three-phase input voltages across the stator terminals to neutral are given by the following equations:

$$v_{as} = r_s i_{as} + \frac{d\lambda_{as}}{dt} \tag{19}$$

$$v_{bs} = r_s i_{bs} + \frac{d\lambda_{bs}}{dt} \tag{20}$$

$$v_{cs} = r_s i_{cs} + \frac{d\lambda_{cs}}{dt} \tag{21}$$

While the magnetically induced rotor three-phase voltages are:

$$v_{ar} = r_r i_{ar} + \frac{d\lambda_{ar}}{dt} \tag{22}$$

$$v_{br} = r_r i_{br} + \frac{d\lambda_{br}}{dt} \tag{23}$$

$$v_{cr} = r_r i_{cr} + \frac{d\lambda_{cr}}{dt} \tag{24}$$

In these equations *v, r, i* and λ represent voltage, resistance, current and flux linkage respectively. The subscripts *a, b* and *c* represent the phases for the voltages and the line currents, while the subscripts *s* and *r* refer to the stator and the rotor.

From (Krause, 1965; Krause, 2002) the flux linkage equations between the stator and rotor are derived from the stator and rotor mutual inductances, as well as the line currents. These flux linkages are given by:

$$\lambda_{as} = L_{asas} i_{as} + L_{asbs} i_{bs} + L_{ascs} i_{cs} + L_{asar} i_{ar} + L_{asbr} i_{br} + L_{ascr} i_{cr} \tag{25}$$

$$\lambda_{bs} = L_{bsas} i_{as} + L_{bsbs} i_{bs} + L_{bscs} i_{cs} + L_{bsar} i_{ar} + L_{bsbr} i_{br} + L_{bscr} i_{cr} \tag{26}$$

$$\lambda_{cs} = L_{csas} i_{as} + L_{csbs} i_{bs} + L_{cscs} i_{cs} + L_{csar} i_{ar} + L_{csbr} i_{br} + L_{cscr} i_{cr} \tag{27}$$

$$\lambda_{ar} = L_{aras} i_{as} + L_{arbs} i_{bs} + L_{arcs} i_{cs} + L_{arar} i_{ar} + L_{arbr} i_{br} + L_{arcr} i_{cr} \tag{28}$$

$$\lambda_{br} = L_{bras}i_{as} + L_{brbs}i_{bs} + L_{brcs}i_{cs} + L_{brar}i_{ar} + L_{brbr}i_{br} + L_{brcr}i_{cr} \quad (29)$$

$$\lambda_{cr} = L_{cras}i_{as} + L_{crbs}i_{bs} + L_{crcs}i_{cs} + L_{crar}i_{ar} + L_{crbr}i_{br} + L_{crcr}i_{cr} \quad (30)$$

In the above equations *L* represents the inductance, *i* represents the current, the subscripts s and r represent the stator and the rotor respectively, and the subscripts a, b and c refer to the phase. For example, L_{bras} represents the inductance between the rotor on phase b and the stator on phase a.

The winding inductances for an induction motor can be represented in matrix form as:

$$L_s = \begin{bmatrix} L_{ls} + L_{ms} & -\frac{1}{2}L_{ms} & -\frac{1}{2}L_{ms} \\ -\frac{1}{2}L_{ms} & L_{ls} + L_{ms} & -\frac{1}{2}L_{ms} \\ -\frac{1}{2}L_{ms} & -\frac{1}{2}L_{ms} & L_{ls} + L_{ms} \end{bmatrix} \quad (31)$$

$$L_r = \begin{bmatrix} L_{lr} + L_{mr} & -\frac{1}{2}L_{mr} & -\frac{1}{2}L_{mr} \\ -\frac{1}{2}L_{mr} & L_{lr} + L_{mr} & -\frac{1}{2}L_{mr} \\ -\frac{1}{2}L_{mr} & -\frac{1}{2}L_{mr} & L_{lr} + L_{mr} \end{bmatrix} \quad (32)$$

$$L_{sr} = L_{sr}\begin{bmatrix} cos\theta_r & cos\left(\theta_r + \frac{2\pi}{3}\right) & cos\left(\theta_r - \frac{2\pi}{3}\right) \\ cos\left(\theta_r - \frac{2\pi}{3}\right) & cos\theta_r & cos\left(\theta_r + \frac{2\pi}{3}\right) \\ cos\left(\theta_r + \frac{2\pi}{3}\right) & cos\left(\theta_r - \frac{2\pi}{3}\right) & cos\theta_r \end{bmatrix} \quad (33)$$

where; L_s, L_r, and L_{sr} refer to the stator inductance, rotor inductance and mutual inductances respectively, while L_{ls} and L_{lr} refer to the stator and rotor leakage inductances and L_{ms} and L_{mr} refer to the stator and rotor magnetising inductances. θ_r represents the angle between the rotor and stator at a certain instance in time.

As it can be seen the flux linkage that enters into the air gap region has two parts and the mutual inductance between the rotor and stator is dependent on the rotor position, so it is depended on the rotor angle. This means the rotor and stator voltage equations are depending on the relative position between the rotor and the stator. Therefore these equations are extremely complicated, which makes modelling of the induction motor

extremely difficult. A change of reference frames, however, greatly simplifies these equations, as is shown in the next section.

2.3 Reference Frame Theory

2.3.1 Introduction

The reference frame theory involves a change of variables in order to simplify the analysis of three-phase machines. As seen earlier in equations (19) to (33), the voltage equations are all differential equations that depend on time. The proposed change of reference frames eliminates these time varying parameters.

A change of variables was first proposed by Robert H. Park in the 1920s. This transformation, known as the Park's transformation involves a change of variables, which transformed the stator variables to a reference frame fixed in the rotor. This transformation eliminates the time varying inductances associated with the voltage equations described in equations (19) to (24). Park defined his voltage equations as (Park, 1929):

$$e_d = \frac{2}{3}\{e_a cos\theta + e_b \cos(\theta - 120) + e_c \cos(\theta + 120)\} \quad (34)$$

$$e_q = \frac{2}{3}\{e_a sin\theta + e_b \sin(\theta - 120) + e_c \sin(\theta + 120)\} \quad (35)$$

$$e_0 = \frac{1}{3}\{e_a + e_b + e_c)\} \quad (36)$$

Where, *e* represents the voltage, the subscripts a, b and c represent the associating phase voltages, and the subscripts d, q and 0 represent the transformed voltages into the dq0 reference frame.

The transformation can be simplified to the matrix convention: $[F_{0dq}] = [P_\theta][F_{ABC}]$

Where: $[P_\theta] = \frac{2}{3}\begin{bmatrix} 1/2 & 1/2 & 1/2 \\ cos\theta & \cos(\theta - \lambda) & \cos(\theta + \lambda) \\ \sin\theta & \sin(\theta - \lambda) & \sin(\theta + \lambda) \end{bmatrix}$ (37)

The zero sequence (e_0) was included to make it possible to invert the transformation and also to handle unbalanced voltages (R. J. Lee, 1984/85).

In the late 1930s Stanley employed a new change of variables to eliminate the time-varying inductances in the voltage equations by transforming the rotor variables to a reference frame fixed in the stator as opposed to Park's transformation which transforms the stator

variables to a reference frame fixed in the rotor. Stanley introduced six new variables; v_α, v_β, v_0, V_α, V_β, and V_0 (Krause, 2002), where:

$$v_\alpha = \frac{2}{3}\left[v_1\, cos\theta + v_2\ cos(\theta + \frac{2\pi}{3}) + v_3\, cos(\theta - \frac{2\pi}{3})\right] \quad (38)$$

$$v_\beta = \frac{2}{3}\left[v_1\, sin\theta + v\ sin(\theta + \frac{2\pi}{3}) + v_3\, sin(\theta - \frac{2\pi}{3})\right] \quad (39)$$

$$v_0 = \frac{1}{3}(v_1 + v_2 + v_3) \quad (40)$$

$$V_\alpha = \frac{2}{3}\left[v_a - \frac{1}{2}(v_b - v_c)\right] \quad (41)$$

$$V_\beta = \frac{\sqrt{3}}{3}(v_b - v_c) \quad (42)$$

$$V_0 = \frac{1}{3}(v_a + v_b + v_c) \quad (43)$$

Kron (Krause, 2002) introduced a transformation which called the synchronously rotating reference frame which transformed both the stator and rotor variables to a reference frame that rotates in synchronism with the rotating magnetic field.

Krause (1965), combined these transformations into one general transformation which eliminates all time-varying inductances by referring the stator and rotor variables to a reference frame that can remain stationary or rotate at any angular velocity. This reference frame is known as the arbitrary reference frame (Krause, 1965; Krause, 2002).

2.3.2 Arbitrary Reference Frame

A transformation into the arbitrary reference frame is defined by the following expression:

$$\mathbf{f}_{qd0s} = \mathbf{K}_s\mathbf{f}_{abcs} \quad (44)$$

$\mathbf{f}_{qd0s}$ represents the variables in the arbitrary reference frame and $\mathbf{f}_{abcs}$ represents the variables in the abc reference frame.

Where:

$$K_s = \frac{2}{3}\begin{bmatrix} \cos(\theta) & \cos(\theta - \frac{2\pi}{3}) & \cos(\theta + \frac{2\pi}{3}) \\ \sin(\theta) & \sin(\theta - \frac{2\pi}{3}) & \sin(\theta + \frac{2\pi}{3}) \\ \frac{1}{2} & \frac{1}{2} & \frac{1}{2} \end{bmatrix}[f_{abcs}]$$

(45)

The inverse transformation is:

$$(K_s)^{-1} = \begin{bmatrix} \cos(\theta) & \sin(\theta) & 1 \\ \cos(\theta - \frac{2\pi}{3}) & \sin(\theta - \frac{2\pi}{3}) & 1 \\ \cos(\theta + \frac{2\pi}{3}) & \sin(\theta + \frac{2\pi}{3}) & 1 \end{bmatrix}[f_{qd0s}] \quad (46)$$

Since, $\omega = \frac{d\theta}{dt}$, $\theta = \int \omega dt$

Where; ω = angular velocity and θ = angular displacement.

This transformation is not only limited to the voltage variables, *f* can also represent current, flux linkages or electric charge. The angular velocity used in the transformation determines the frame of reference the variables are being transformed into. The three most common transformations are: a transformation into the stationary reference frame, where the angular velocity is set to zero, this is commonly known as the Clark's transformation; a transformation into the rotor reference frame, where the angular velocity is the velocity of the rotor and is known as the Park's transformation (Park, 1929), and a transformation into the synchronous reference frame, where the angular velocity is set to the synchronous speed (Krause, 2002).

2.3.3 Commonly Used Reference Frames

2.3.3.1 Stationary Reference Frame 0

For the stationary reference frame the stationary circuit variables are referred to the stationary reference frame where the reference frame speed is zero, meaning the d and q axes do not rotate. The stationary reference frame was developed by Clark, known as the Clark's transformation. This transformation uses the notation; f_α, f_β and f_0 for the transformed variables

The stationary reference frame can be thought of as projecting three-phase voltages (or currents) varying in time along the a, b, and c phase axes onto two-phase voltages varying in time along a pair of orthogonal axes ds and qs fixed on the stator. It is often convenient to assume that one of the stationary variables is collinear with the a-axis, as shown in figure 3.

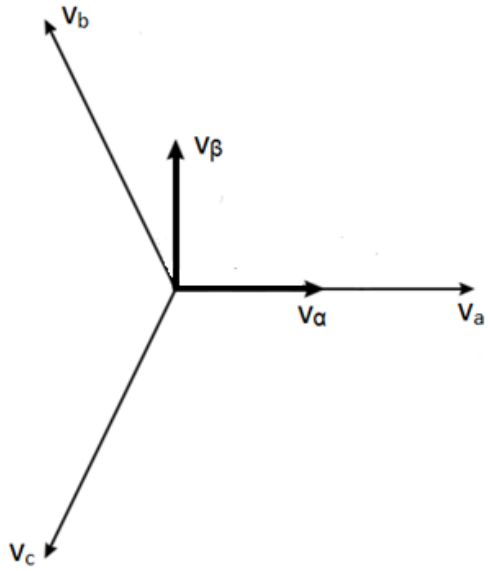

Figure 3: Geometric representation of the stationary reference frame.

Since the angular velocity is zero, the transformation becomes:

$$\begin{bmatrix} f_\alpha \\ f_\beta \\ f_0 \end{bmatrix} = \frac{2}{3}\begin{bmatrix} 1 & -\frac{1}{2} & -\frac{1}{2} \\ 0 & \frac{\sqrt{3}}{3} & \frac{-\sqrt{3}}{3} \\ \frac{1}{2} & \frac{1}{2} & \frac{1}{2} \end{bmatrix}\begin{bmatrix} f_a \\ f_b \\ f_c \end{bmatrix} \quad (47)$$

Where the subscripts α, β, and 0 refer to the variables in the stationary reference frame.

If the abc variables are balanced, then $f_0 = 0$ and, therefore, the transformation will reduce the three input variables into two orthogonal variables as shown in figure 3.

2.3.3.2 Reference Frame Fixed in the Rotor ω_r

The stationary variables are referred to a reference frame fixed in the rotor. So the reference frame speed is that of the rotor speed.

An important concept underlying the rotor reference frame is that in the induction machine, the rotor is also a three-phase system. Therefore, it too will have an a-phase axis. The rotor

reference frame will maintain its d-axis collinear with the axis of the rotor a-phase, as seen in figure 4. The speed of rotation of this reference frame is ω_r.

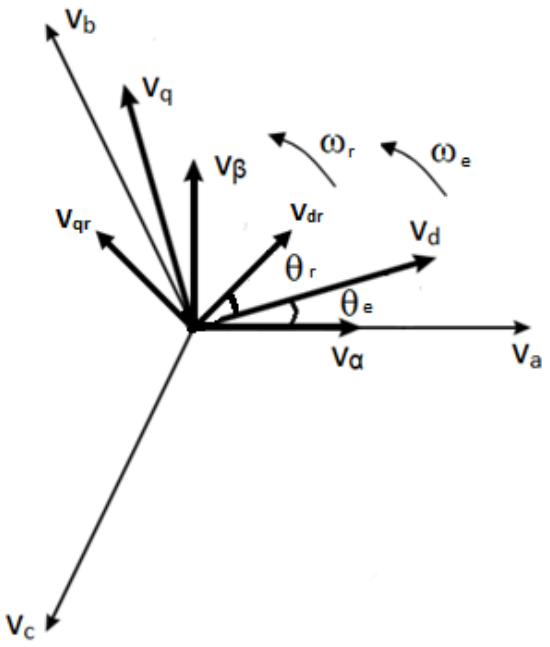

Figure 4: Geometric representation of the rotor reference frame.

Projection of a vector expressed in the stationary reference frame qs-ds into the rotor reference frame qr-dr is obtained via:

$$\begin{bmatrix} v_q^r \\ v_d^r \end{bmatrix} = \begin{bmatrix} \cos(\theta_e + \theta_r) & -\sin(\theta_e + \theta_r) \\ \sin(\theta_e + \theta_r) & \cos(\theta_e + \theta_r) \end{bmatrix} \begin{bmatrix} v_q^s \\ v_d^s \end{bmatrix} \quad (48)$$

2.3.3.3 Synchronously Rotating Reference Frame ω_e

The stationary variables are referred to synchronously rotating reference frame, so the reference frame speed is that of synchronous speed, as seen in figure 5.

The synchronous reference frame corresponds to a rotating reference frame moving at synchronous speed, denoted by ω_e.

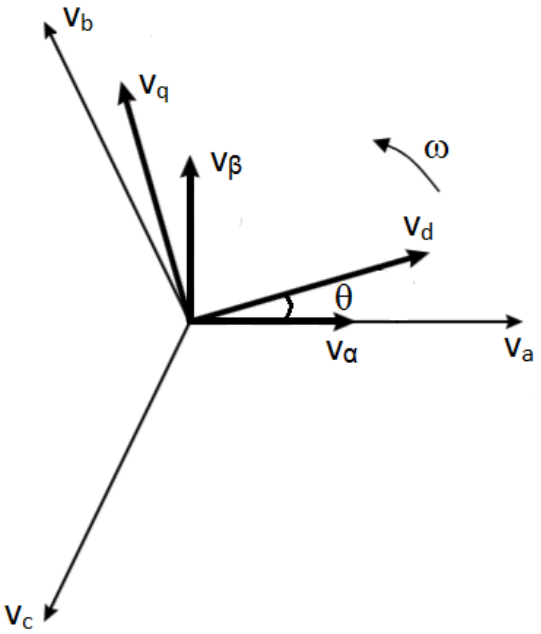

Figure 5: Geometric representation of the synchronouse reference frame.

Projection of a vector expressed in the stationary reference frame qs-ds into the synchronous reference frame qe-de is obtained via:

$$\begin{bmatrix} v_q^e \\ v_d^e \end{bmatrix} = \begin{bmatrix} cos\theta & -sin\theta \\ sin\theta & cos\theta \end{bmatrix} \begin{bmatrix} v_q^s \\ v_d^s \end{bmatrix} \quad (49)$$

2.3.4 Arbitrary Reference Frame Equations

The equations used to analyse a three-phase induction motor can be derived from the equivalent circuit of an induction motor in the arbitrary reference frame, as seen in figure 6.

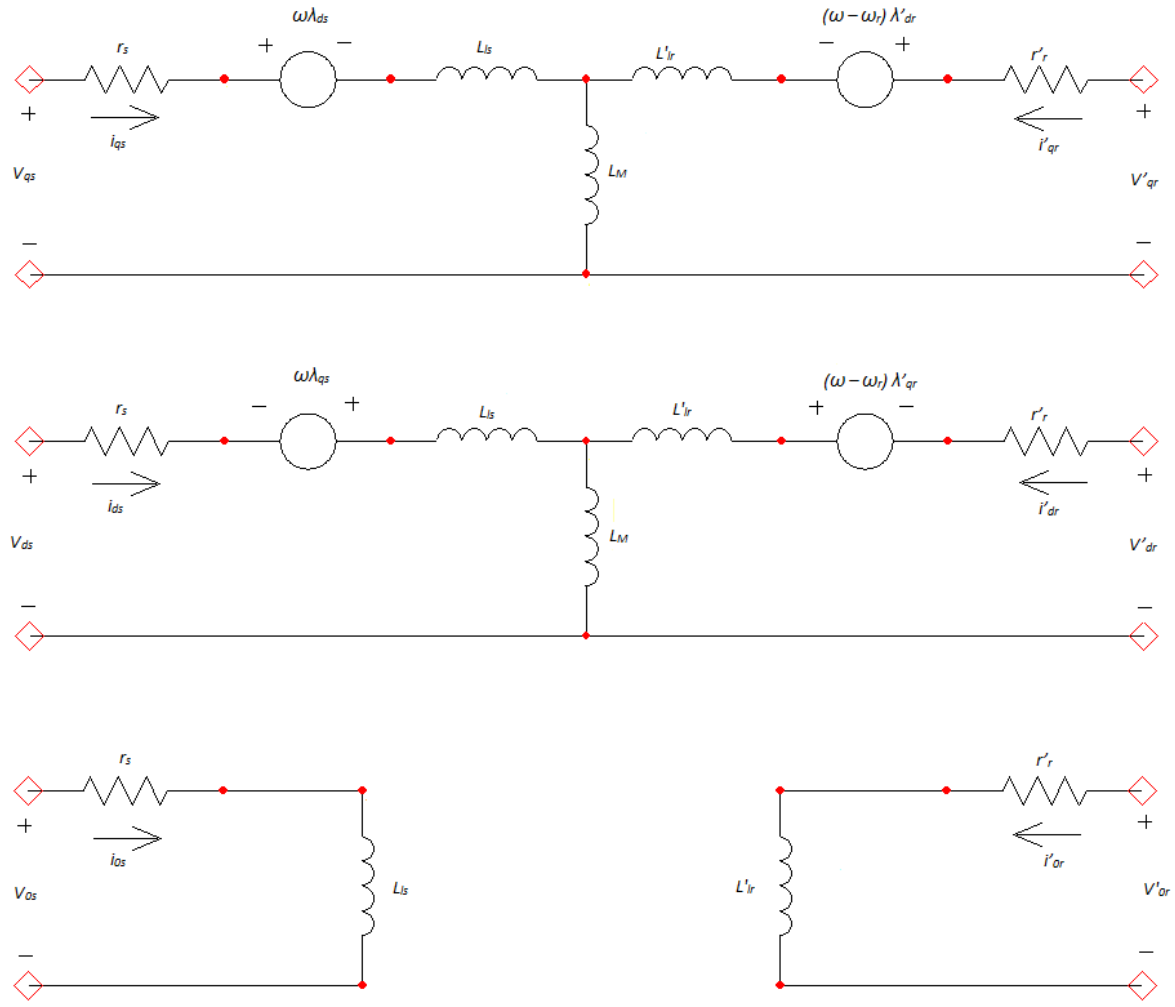

Figure 6: Equivalent Circuit of an Induction Motor in the Arbitrary Reference Frame.

From the above figure, the flux linkage equations can be solved as:

$$\frac{d\psi_{qs}}{dt} = \omega_b \left[v_{qs} - \frac{\omega_e}{\omega_b}\psi_{ds} + \frac{R_s}{X_{ls}}\left(\psi_{mq} - \psi_{qs}\right)\right] \quad (50)$$

$$\frac{d\psi_{ds}}{dt} = \omega_b \left[v_{ds} - \frac{\omega_e}{\omega_b}\psi_{qs} + \frac{R_s}{X_{ls}}\left(\psi_{md} - \psi_{ds}\right)\right] \quad (51)$$

$$\frac{d\psi_{qr}}{dt} = \omega_b \left[v_{qr} - \frac{\omega_e}{\omega_b}\psi_{dr} + \frac{R_s}{X_{ls}}\left(\psi_{mq} - \psi_{qr}\right)\right] \quad (52)$$

$$\frac{d\psi_{dr}}{dt} = \omega_b \left[v_{dr} - \frac{\omega_e}{\omega_b}\psi_{qr} + \frac{R_s}{X_{ls}}(\psi_{md} - \psi_{dr}) \right] \quad (53)$$

where:

$$\psi_{mq} = X_{ml}\left[\frac{\psi_{qs}}{X_{ls}} + \frac{\psi_{qr}}{X_{lr}}\right] \quad (54)$$

$$\psi_{md} = X_{ml}\left[\frac{\psi_{ds}}{X_{ls}} + \frac{\psi_{dr}}{X_{lr}}\right] \quad (55)$$

$$X_{ml} = \frac{1}{\left[\frac{1}{X_{ls}} + \frac{1}{X_{lr}} + \frac{1}{X_m}\right]} \quad (56)$$

From the flux linkage equations the current equations can be determined:

$$i_{qs} = \frac{1}{X_{ls}}\left(\psi_{qs} - \psi_{mq}\right) \quad (57)$$

$$i_{ds} = \frac{1}{X_{ls}}(\psi_{ds} - \psi_{md}) \quad (58)$$

$$i_{qr} = \frac{1}{X_{lr}}\left(\psi_{qr} - \psi_{mq}\right) \quad (59)$$

$$i_{dr} = \frac{1}{X_{ls}}(\psi_{dr} - \psi_{md}) \quad (60)$$

From the current and flux equations the equations for the torque and rotor speed can be determined as:

$$T_e = \left(\frac{3}{2}\right)\left(\frac{P}{2}\right)\left(\frac{1}{\omega_b}\right)\left(\psi_{ds}i_{qs} - \psi_{qs}i_{ds}\right) \quad (61)$$

$$\omega_r = \int \frac{P}{2J}(T_e - T_L) \quad (62)$$

Where P is the number of poles and J is the moment of inertia.

2.4 Induction Motor Equivalent Circuit Parameter Tests

2.4.1 Introduction

The equivalent circuit for an induction motor is a useful tool to determine its performance (Chapman, 2012). There are many proposed methods to calculate or estimate the circuit parameters for an induction motor, which are; R_1, R_2, X_1, X_2 and X_M. The most common

methods are the DC test, blocked-rotor test and the no-load test (Chapman, 2012; Paul C. Krause, 2002).

2.4.2 DC Test

The DC Test determines the stator resistance, R_1. It is performed by applying a DC voltage through two of the three phases at the motor's rated current. The DC test is performed at the rated current in order to heat the windings to their operational temperature for more accurate results. A DC current is used because it will not induce a voltage onto the rotor and, therefore, the stator resistance can be accurately measured (Chapman, 2012). The input voltage is recorded along with the current and using Ohms law the stator resistance can be calculated. Since the measured currents and voltages are across two phases. The equation for a wye-connected stator resistance becomes: $2R_1 = \frac{V_{DC}}{I_{DC}}$ or $R_1 = \frac{V_{DC}}{2I_{DC}}$, while for a delta-connected stator, the equation for the resistance becomes: $R_1 = (\frac{3}{2})\frac{V_{DC}}{I_{DC}}$.

This test is effective because of its simplicity. However, it is not completely accurate because it does not account for the skin effect (The Institute of Electrical and Electronic Engineers, Inc., 1996). The skin effect occurs when ac electricity is run through a conductor, the flow of current tends to remain on the outer periphery of the conductor and is more prominent for higher frequencies. This results in the resistance being larger than first expected because the flow of electrons is not utilising all of the cross-sectional area the conductor.

2.4.3 No-Load Test

The no-load test is very much like the open circuit test of a transformer. It gives information on the magnetization current and the rotational losses. The test is performed by applying a balanced three-phase source to the motor at its rated voltage and frequency while it is on no load. The motor will rotate at almost synchronous speed meaning that the slip is very close to zero. This means that the rotor resistance, $\frac{R_2}{s} \approx \infty$, therefore the rotor part of the circuit can be neglected because it can be assumed that all of the current will flow through R_C and X_M, as shown in Figure 8 below (Chapman, 2012).

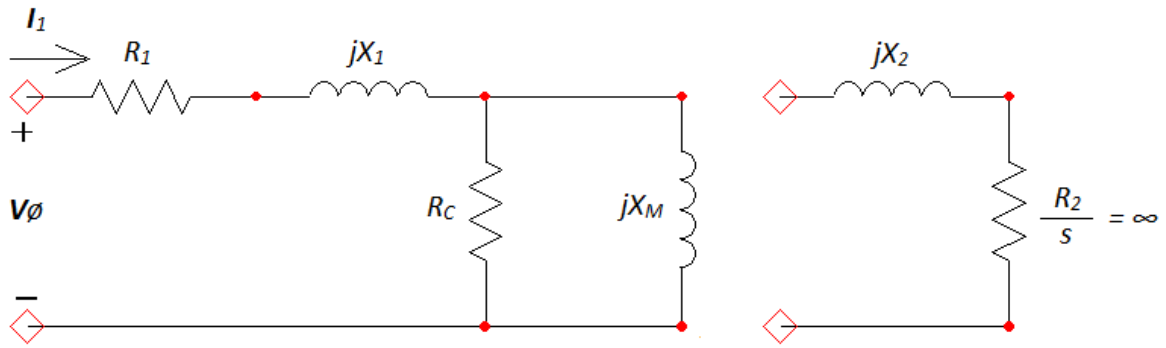

Figure 8: Equivalent Circuit for the No-Load Test Performed on an Induction Motor.

2.4.4 Blocked (Locked) Rotor Test

The blocked rotor test corresponds to the short-circuit test of a transformer. It provides information on the leakage impedance and rotor resistance. For this test the rotor is blocked so that it cannot move. This test is performed at the motors rated current value with the frequency limited to 20 – 25% of the rated frequency (The Institute of Electrical and Electronic Engineers, Inc., 1996). This is because under normal operating conditions the slip of most motors is around 2 – 4%, and therefore, the resulting rotor frequency is around 1 – 3 Hz (Chapman, 2012).The voltage, current and power are then measured. During the blocked rotor test the slip is equal to 1, and therefore the rotor resistance (R_2) is not dependant on the slip and is small compared to R_C and X_M. Therefore, it is reasonable to assume that all of the current will flow through R_2 and neglect the other elements, as shown in the schematic diagram of figure 9:

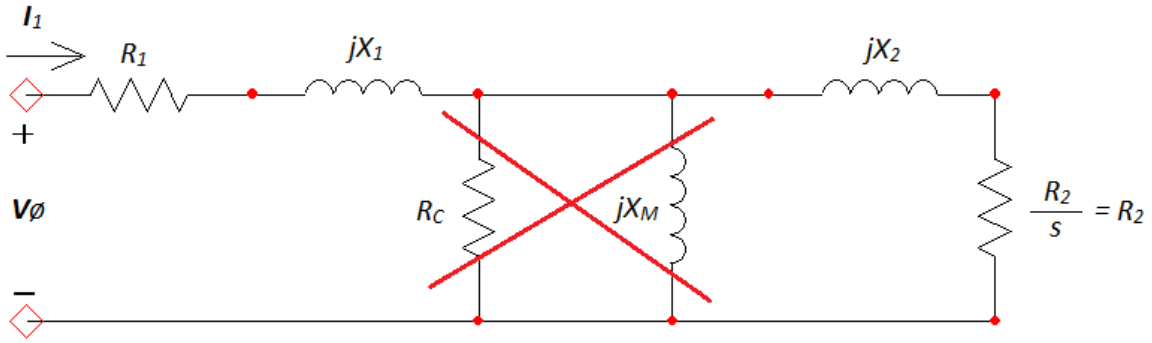

Figure 9: Equivalent Circuit for the Blocked Rotor Test Performed on an Induction Motor.

During this test, the power, frequency, line current and the phase voltage are recorded.

2.5 Determination of Equivalent Circuit Parameters from Tests

There are a few alternate methods proposed to determine the equivalent circuit parameters of a three-phase induction motor. The methods do not differ greatly, however one method could be more accurate than the other based on the type of motor, the tests performed and the results obtained.

2.5.1 Method 1

The method described in (Chapman, 2012) first determines the stator resistance R_1 from the DC test where:

$$R_1 = \frac{V_{DC}}{2I_{DC}} \; or \; \frac{2}{3}\frac{V_{DC}}{I_{DC}} \tag{63}$$

depending on whether the stator is wye connected or delta connected.

Then the no-load impedance, $|Z_{NL}|$, and the blocked rotor impedance, $|Z_{BR}|$, are determined by dividing their recorded per phase voltages by their corresponding line currents and using Ohms law, assuming a wye connected stator:

$$Z = \frac{V_\phi}{I_1} \tag{64}$$

The impedance angle is then determined by using the apparent power, along with the recorded active power, into the equation:

$$\theta = cos^{-1}\left(\frac{P_{in}}{\sqrt{3}V_{NL}I_{NL}}\right) \tag{65}$$

where V_{NL} and I_{NL} refer to the line voltage and current under no load respectively.

The impedance angle is then used to determine the blocked-rotor resistance, the no-load resistance and the blocked-rotor reactance:

$$R_{BR} = |Z_{BR}|cos\theta \tag{66}$$

$$R_{NL} = |Z_{NL}|cos\theta \tag{67}$$

$$X'_{BR} = |Z_{BR}|cos\theta \quad (68)$$

From the per phase equivalent circuit under blocked rotor conditions it can be seen that:

$$R_{BR} = R_1 + R_2 \quad (69)$$

Since R_1 and R_{BL} have already been determined R_2 can be easily calculated.

The calculated blocked-rotor reactance is then transformed to its equivalent value at the rated frequency:

$$X_{BR} = \frac{f_{rated}}{f_{measured}} X'_{BR} \quad (70)$$

X_1 and X_2 can then be determined through the use of the NEMA design class table (Chapman, 2012), shown in figure 1 below.

Table 1: NEMA design class table for estimating stator and rotor reactances for a three-phase induction motor

	Xs (% of Xeq)	*Xr (% of Xeq)*
Wound Rotor	50	50
Class A	50	50
Class B	40	60
Class C	30	70
Class D	50	50

From the value of X_1, the magnetising reactance, X_M can be calculated from:

$$X_M = |Z_{NL}| - X_1.$$

2.5.2 Method 2

From the no-load test:

$$|Z_{eq}| = \frac{V_\emptyset}{I_{1,nl}} \approx X_1 + X_M \quad (71)$$

$$S_{NL} = V_{NL} I_{NL} \quad (72)$$

$$S_{NL} = \sqrt{P_{NL}^2 + Q_{NL}^2} \quad (73)$$

$$Q_{NL} = \sqrt{S_{NL}^2 - P_{NL}^2} \quad (74)$$

$$Q_{NL} = I_{NL}^2 X_{NL} \quad (75)$$

$$X_{NL} = \frac{Q_{NL}}{I_{NL}^2} \quad (76)$$

$$X_{NL} = X_1 + X_M \quad (77)$$

Substitute X_1 from the blocked-rotor test to determine X_M.

From the blocked-rotor test:

$$|Z_{eq}| = \frac{V_{\emptyset}}{I_1} \quad (78)$$

$$R_{BR} = R_1 + R_2 \quad (79)$$

$$R_{BR} = \frac{P_{BR}}{I_{BR}^2} \quad (80)$$

$$R_2 = R_{BR} + R_1 \quad (81)$$

$$|Z_{BR}| = \sqrt{R_{BR}^2 + X_{BR}^2} \quad (82)$$

$$X_{BR} = \sqrt{Z_{BR}^2 - R_{BR}^2} \quad (83)$$

$$X_{BR,real} = \frac{f_{rated}}{f_{measured}} X_{BR} \quad (84)$$

$$X_{BR,real} = X_1 + X_2 \quad (85)$$

2.6 Simulation of a Three-Phase Induction Motor

A simulation gives an accurate depiction of the transient and steady-state behaviour of the motor. It is often advantageous to employ a change of reference frames in order to simplify the simulation and save on computer processing time. Perhaps the first published article outlining this technique was employed in (Krause, 1965). The paper outlined the importance of simulating three-phase induction machines as the behaviour of these machines has an important effect on the performance of the electrical system of which they are a part. This paper outlines the equations used for the simulation of three-phase induction machines in the arbitrary reference frame. The simulation results of the behaviour of two-phase and three-phase induction machines during balanced and unbalanced conditions are presented.

Lee (1984/85) presents the equations used for the simulation of an induction motor for three of the most popular reference frames; the stationary reference frame, the rotor reference frame and the synchronous reference frame. Any of the three reference frames can be used to predict an induction motor's transient behaviour.

The stationary reference frame is the simplest of the three; it does not involve an inverse Park's transformation in order to obtain the stator variables, and therefore saves on computer time. It is also the most useful when the analysis is confined to the stator variables, like variable speed stator fed induction motor drives.

Rotor reference frame saves computer time because it eliminates the need to perform an inverse transformation to obtain the rotor phase variables. It is useful when the analysis is interested in only the rotor variables, as in variable speed rotor fed induction motor drives.

Synchronous reference frame is found to be the preferred reference frame for simulating induction motors because it creates DC quantities in both the rotor and stator d,q variables. This means that the integration step employed in the simulation may be lengthened without affecting the accuracy of the results.

This paper proposes an equivalent circuit for the mechanical aspect of a three-phase induction machine. It uses the equivalent circuit derived in (Krause, 1965) along with its own equivalent circuit to represent the mechanical aspect of an induction motor. The simulation is composed in an electrical circuit simulator, Simplorer. This method is not needed for the simulation in the computer program MATLAB/Simulink because the mechanical aspect of an induction motor can be accurately depicted by function blocks and mathematical implementations. The method proposed by this paper was compared to the simulation results from (Krause, 2002) and found to be extremely accurate.

MATLAB/Simulink seems to be the preferred computer program used for the simulation of three-phase induction machines with many forms of literature outlining various methods. Orille (1999) perhaps proposed the first MATLAB/Simulink implementation of the simulation of three-phase induction machines. They implemented the simulation using the method proposed in (Krause, 1965). The findings from the paper indicated that the

MATLAB/Simulink program proved to be capable of simulating the transient and steady-state characteristics of three-phase induction machines with different reference frames.

The method proposed by Shah (2012) compared the results of the torque and speed characteristics in different reference frames; the stationary reference frame, the rotor reference frame and the synchronous reference frame. The simulation was achieved by first implementing a change of reference frame from the three-phase input voltages and then used the flux, current, torque and speed equations described in (Krause, 2002) to simulate the motor. The torque and speed characteristics for all reference frames were found to be identical which indicates that these characteristics do not depend on the selection of reference frame. However the type of reference frame being used does determine the shape and frequency of the waveforms for the stator voltages and currents, where they have DC characteristics in the synchronous reference frame and sinusoidal characteristics in the rotor and stationary reference frames.

Shah (2012) used MATLAB/Simulink to simulate a three-phase induction motor in the synchronous reference frame under different load conditions. The author also used the equations for the simulation from (Krause, 1965). The model was set so that the user could vary the machine variables and analyse the standard characteristics as well as the characteristics of the motors flux. The author, Shah, believes that Simulink is a key tool for the teaching and research purposes of electrical machine drive systems.

Boora (2013) also uses the equations proposed in Krause (1965) to simulate a three-phase induction motor. Again the simulation is used to explore the effects that mechanical loading has on the motor's standard characteristics. The author shows that a reference frame transformation is extremely advantageous for the simulation of three-phase induction motors. However, Boora believes that there are limitations within this method of direct starting of induction machines and the effect that varying mechanical loads have on various characteristics of the motor.

Ghanim (2011), Khorasani (2008), Wadhwani, Sandhu (2009), Tolbert (2003), L.G (2010) Bilgin (2012) all implement the same mathematical model proposed in Krause (1965) to simulate three-phase induction machines in MATLAB/Simulink. Although their simulations

do differ slightly, all of their results conclude that MATLAB/Simulink is a very powerful and reliable tool that can be used to analyse the behaviour of three-phase induction machines. Bilgin (2012) differs slightly from the rest in allowing the user to define variables associated to the rotor bars and the end-rings of the machine.

3 Methodology

Before commencing the equivalent circuit parameter tests on the motor the motors rated parameters must be known. These can be determined from the nameplate data as shown in figure 10. As we can see the motors stator is wye connected and it has a rated voltage of 415 V which equates to a phase voltage of 240 V. The rated frequency is 50 Hz, rated speed is 1375 rpm, rated power is 0.37 kW and the rated current is 1.02 A. It is a four pole machine so from equation 1 synchronous speed is 1500 rpm.

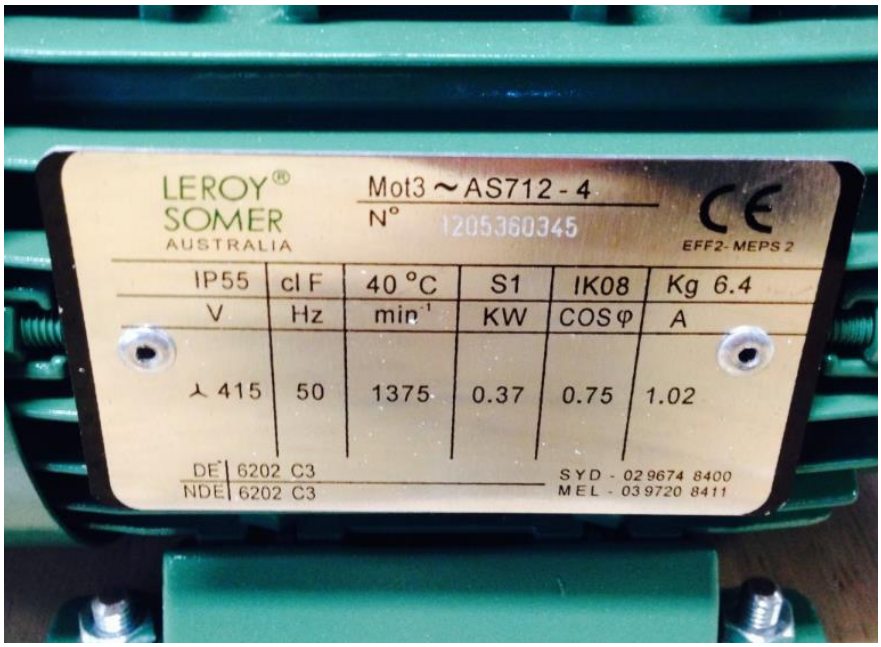

Figure 10: Nameplate data of motor used

3.1 DC Test

3.1.1 Equipment

- Variable DC power supply
- Cables
- Three-phase induction motor
- Digital multimeter

3.1.2 Method

The DC power supply was connected across two of the phase windings, phase a and phase b, and set to vary the input current. The required DC current was 1.02 amps.

Upon the first attempt the DC power supply was set to independent. It was found that with the maximum DC voltage and current applied through the stator the maximum voltage that could be applied was 30 V DC. This equated to a current flow of only approximately 0.65 amps.

The DC power supply was then connected in series in order to double the maximum level for the applied voltage, 60 V DC max.

Upon the second test, the required DC current of 1.02 amps was reached.

The DC power supply was then used to determine the voltage being applied. This was 24.7 V DC for both the slave and master units. Therefore since two voltages sources are applied in series the total voltage is the sum of both, 49.4 V DC.

A digital multimeter was connected across the two phases being measured to validate this value.

This test was repeated for phases a to c and b to c.

3.2 No-load test

3.2.1 Equipment

- MOVITRAC® 07 frequency Inverter (VSD)
- WT2030 Digital Power Meter
- Three-phase induction motor

3.2.2 Method

The VSD fed power through the three-phase power meter which was connected to the three-phase induction motor.

The VSD was set to run the motor at the rated values of 50 Hz and 415 V line-to-line with the motor running at its rated 1375 rpm.

The power meter was set to measure the apparent power across all phases, the per-phase voltage, the line current and the frequency.

Upon the first attempt it was found that the VSD could only apply a maximum voltage of 230 V with a frequency of approximately 45 Hz. For this test it is advantageous to use the rated voltage and frequency (The Institute of Electrical and Electronic Engineers, Inc., 1996).

This problem was rectified by bypassing the VSD and running the system directly from the mains supply which in Australia is 240 V line-to-neutral, which equals a line-to-line voltage of 415 V, and 50 Hz.

The power, voltage and current were then measured.

There seemed to be a problem with the power meter, it was displaying the active power with negative values. This problem was rectified by reversing two of the phase inputs to the power meter.

The values were again measured.

3.3 Blocked-rotor test

3.3.1 Equipment

- MOVITRAC® 07 frequency Inverter (VSD)
- WT2030 Digital Power Meter
- Three-phase induction motor
- Screws for coupling the motors
- A bracket to block the motors rotating

3.3.2 Method

The VSD fed power through the three-phase power meter which was connected to the three-phase induction motor being measured.

The first step was to block the motors rotor. This was done by screwing a bracket to the end of the rotor which was aligned sitting level with the table the motor was connected to.

The speed of the VSD was set to its minimum position and increased slowly until the rated current of the motor, 1.02 A, was reached. This was determined through the line current measurement on the power meter.

The voltage, current, power and frequency were promptly noted down. Under blocked rotor conditions it is not advisable to run the motor for too long otherwise you run the risk of overheating the motor.

This test was repeated several times.

3.4 Moment of inertia tests

This test was to calculate the moment of inertia in the motor being analysed. It was performed in two stages. The first test was to determine the power consumed in the motors rotor and the second test was to determine the deceleration characteristics of the motor.

3.4.1 Equipment

- WT2030 Digital Power Meter
- 2x Three-phase induction motors
- Screws for coupling the motors
- Tachometer
- Stopwatch

3.4.2 Method for power test

Again the VSD was bypassed for this test.

Three-phase power was applied to the second motor while coupled to the motor under test, and was run with its rated voltage and frequency.

The power consumed by the second motor was measured from the power meter connected across all phases.

The motors were then decoupled and power was supplied to the second motor, this time under no load conditions.

The power being consumed across all phases was measured with the power meter.

3.4.3 Method for deceleration test

The motor under test was powered from the three phase power supply and run at a speed higher than its rated speed of 1375 revs/min. This was achieved again by bypassing the VSD

and applying the three-phase mains power directly to the motor. This allowed the motor to reach a speed of close to synchronous speed, 1500 revs/min.

A white reflective strip was attached to the rotor and the speed of the rotor was measured using a tachometer.

The power to the motor under test was quickly switched off and the time the rotor took to come to a halt was recorded using a stopwatch while the decrease in speed for different time intervals was recorded from the tachometer.

It was found that the motor would stop in less than 1.5 seconds. This proved an issue in trying to determine the rotors speed with the tachometer. It was not physically possible to read the tachometers values in this short time.

A video camera was then set up to record the values being displayed by the tachometer.

The test was performed and recorded several times.

The captured video and audio footage was then analysed to determine the rotor speed with respect to time.

3.5 Simulation of a Three-Phase Induction Motor using MATLAB/Simulink

For the simulation, the synchronously rotating reference frame was chosen, this is because such a reference frame for a balanced three-phase supply results in two DC quantities.

The model was broken down into 4 main parts; Park's transformation, flux and current equations, then inverse Park's transformation and torque and speed calculations.

The equations for the induction motor model can be derived from the equivalent circuit model shown in Figure 6.

The flux linkage equations can be solved as:

$$\frac{d\psi_{qs}}{dt} = \omega_b \left[v_{qs} - \frac{\omega_e}{\omega_b}\psi_{ds} + \frac{R_s}{X_{ls}}(\psi_{mq} - \psi_{qs}) \right]$$

$$\frac{d\psi_{ds}}{dt} = \omega_b \left[v_{ds} - \frac{\omega_e}{\omega_b}\psi_{qs} + \frac{R_s}{X_{ls}}(\psi_{md} - \psi_{ds}) \right]$$

$$\frac{d\psi_{qr}}{dt} = \omega_b \left[v_{qr} - \frac{\omega_e}{\omega_b}\psi_{dr} + \frac{R_s}{X_{ls}}(\psi_{mq} - \psi_{qr}) \right]$$

$$\frac{d\psi_{dr}}{dt} = \omega_b \left[v_{dr} - \frac{\omega_e}{\omega_b}\psi_{qr} + \frac{R_s}{X_{ls}}(\psi_{md} - \psi_{dr}) \right]$$

Where:

$$\psi_{mq} = X_{ml}\left[\frac{\psi_{qs}}{X_{ls}} + \frac{\psi_{qr}}{X_{lr}}\right]$$

$$\psi_{md} = X_{ml}\left[\frac{\psi_{ds}}{X_{ls}} + \frac{\psi_{dr}}{X_{lr}}\right]$$

$$X_{ml} = \frac{1}{\left[\frac{1}{X_{ls}} + \frac{1}{X_{lr}} + \frac{1}{X_m}\right]}$$

From the flux linkage equations the current equations can be determined:

$$i_{qs} = \frac{1}{X_{ls}}(\psi_{qs} - \psi_{mq})$$

$$i_{ds} = \frac{1}{X_{ls}}(\psi_{ds} - \psi_{md})$$

$$i_{qr} = \frac{1}{X_{lr}}(\psi_{qr} - \psi_{mq})$$

$$i_{dr} = \frac{1}{X_{ls}}(\psi_{dr} - \psi_{md})$$

From the current and flux equations the equations for the torque and rotor speed can be determined as:

$$T_e = \left(\frac{3}{2}\right)\left(\frac{P}{2}\right)\left(\frac{1}{\omega_b}\right)(\psi_{ds} i_{qs} - \psi_{qs} i_{ds})$$

$$\omega_r = \int \frac{P}{2J}(T_e - T_l)$$

where P is the number of poles and J is the moment of inertia.

The balanced three-phase stator voltages can be expressed as:

$$V_a = \sqrt{2}V_{rms}sin(\omega t)$$

$$V_b = \sqrt{2}V_{rms}sin\left(\omega t - \frac{2\pi}{3}\right)$$

$$V_c = \sqrt{2}V_{rms}sin\left(\omega t + \frac{2\pi}{3}\right)$$

The next step is to transform these voltages into the stationary reference frame using Clark's transformation. This was done by using the matrix equation:

$$\begin{bmatrix} V_\alpha \\ V_\beta \end{bmatrix} = \begin{bmatrix} \frac{2}{3} & \frac{-1}{3} & \frac{-1}{3} \\ 0 & \frac{\sqrt{3}}{3} & \frac{-\sqrt{3}}{3} \end{bmatrix} \begin{bmatrix} V_a \\ V_b \\ V_c \end{bmatrix}$$

Then the values were transformed into the synchronous reference frame by:

$$\begin{bmatrix} v_q^e \\ v_d^e \end{bmatrix} = \begin{bmatrix} cos\theta_e & sin\theta_e \\ sin\theta_e & -cos\theta_e \end{bmatrix} \begin{bmatrix} V_\alpha \\ V_\beta \end{bmatrix}$$

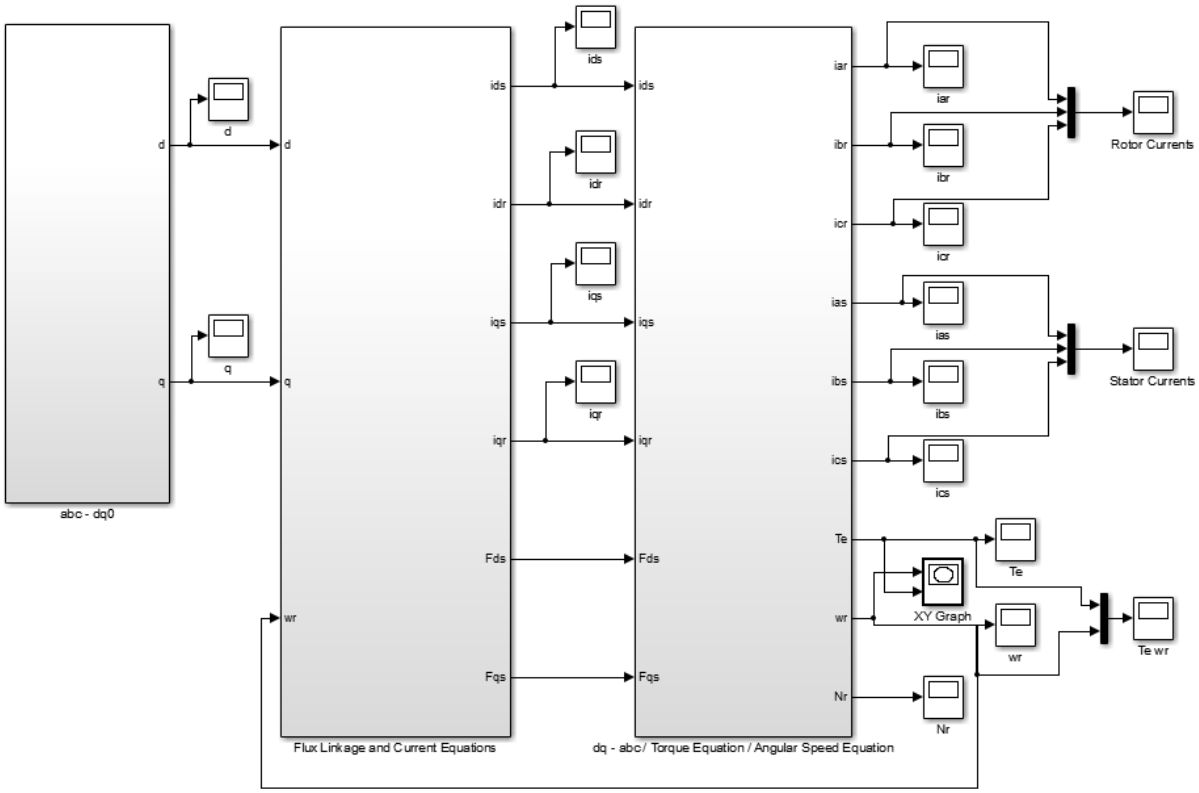

Figure 11: Three-Phase Induction Motor MATLAB/Simulink Model

To perform the Park's transformation, a balanced three-phase voltage source was generated. The resulting three phase voltages were into a stationary reference frame using Clark's transformation (equation 47). Then equation 49 was used to finally transform the voltages into the synchronous reference frame. To generate the angular velocity for the synchronous reference frame a repeating sequence was produced to generate the values for synchronous speed, as shown in figure 12.

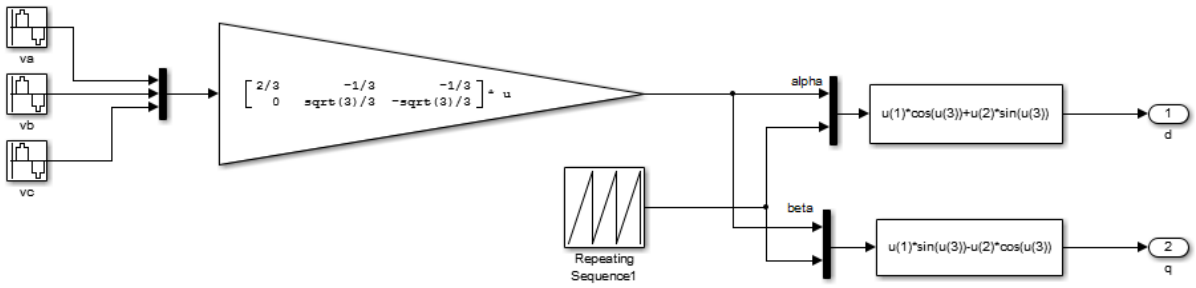

Figure 12: Transformations of reference frames associated with the supply voltages

Figure 13 shows the function blocks associated with the 'Flux linkage and Current Equations' function box from figure 11. Figures 14 and 15 represent the implementation of the flux linkage equations (equations 50 to 56). While figure 16 shows the current equations.

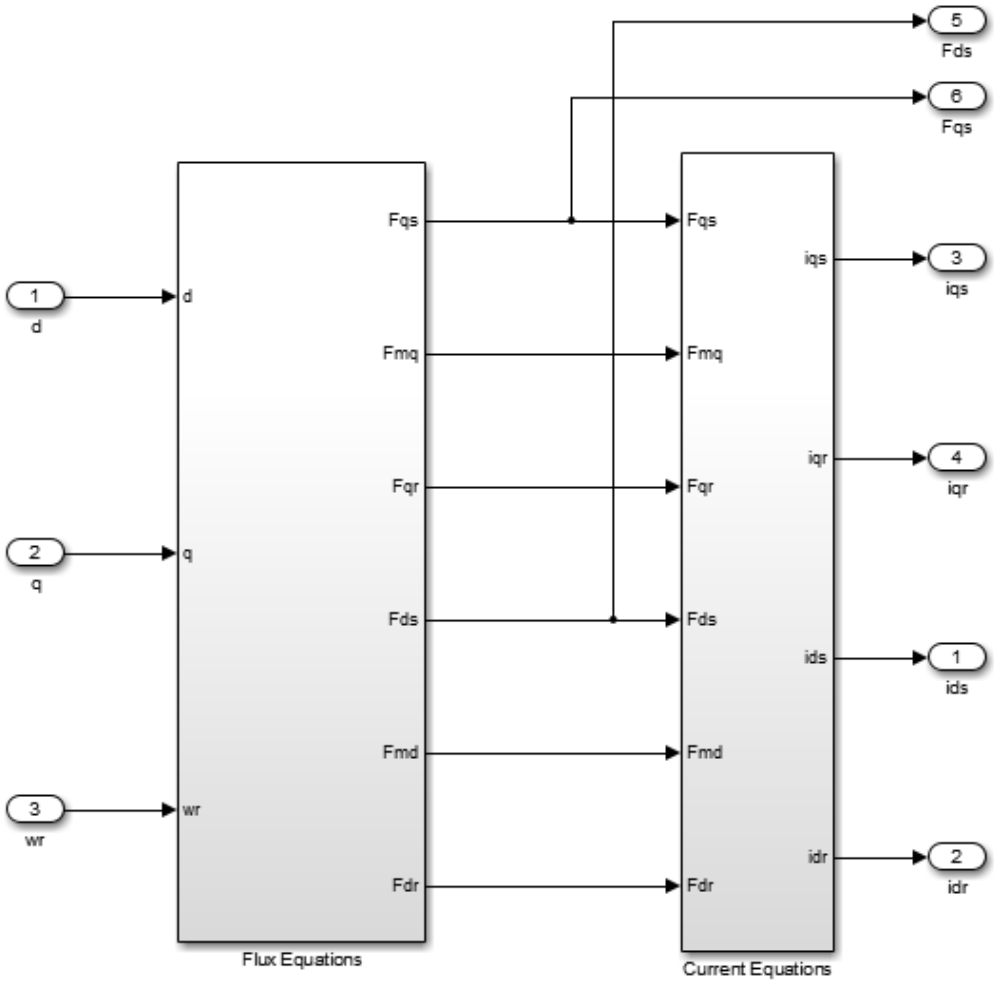

Figure 13: Function blocks for flux and current equations

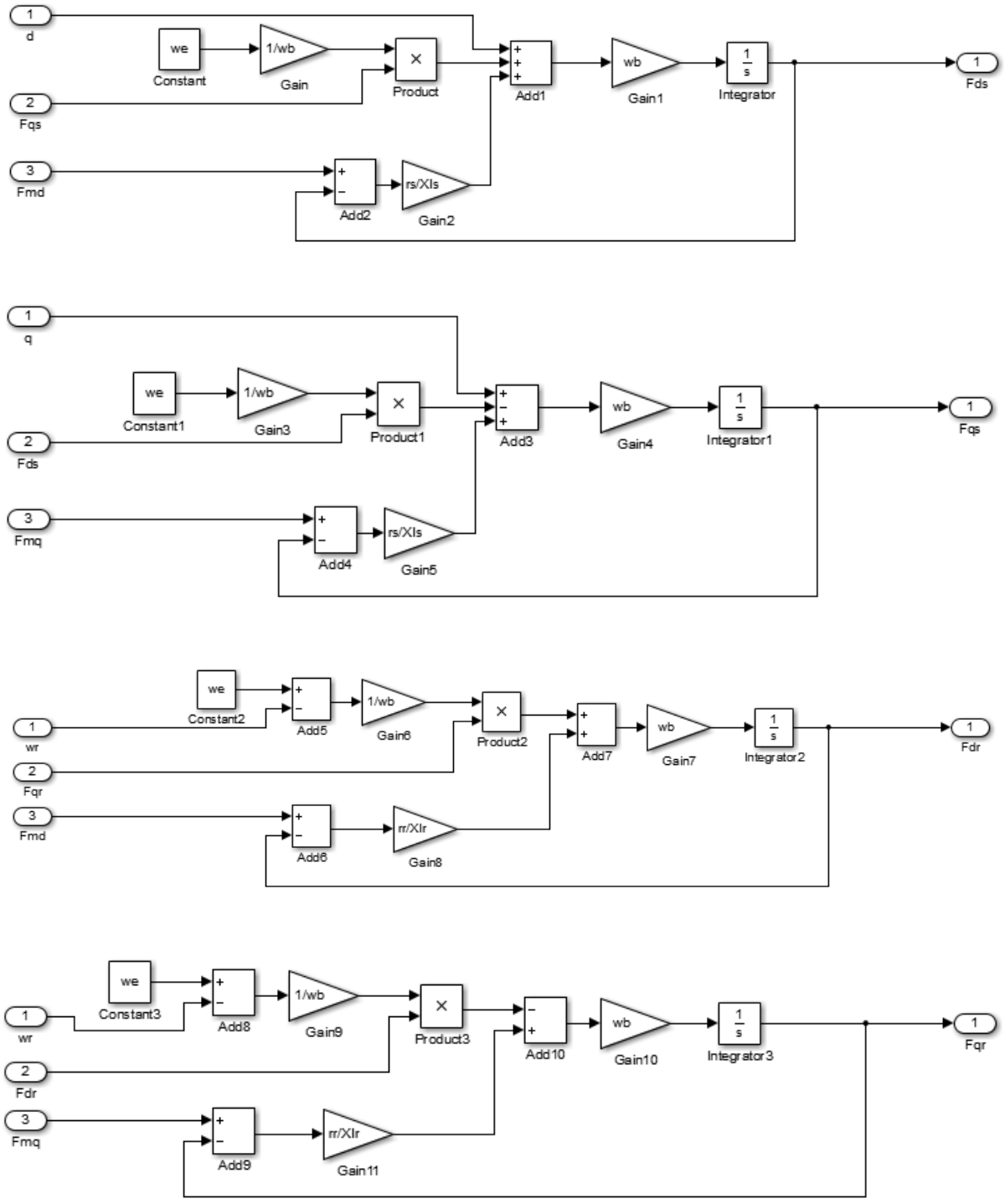

Figure 14: Implementation of flux linkage equations

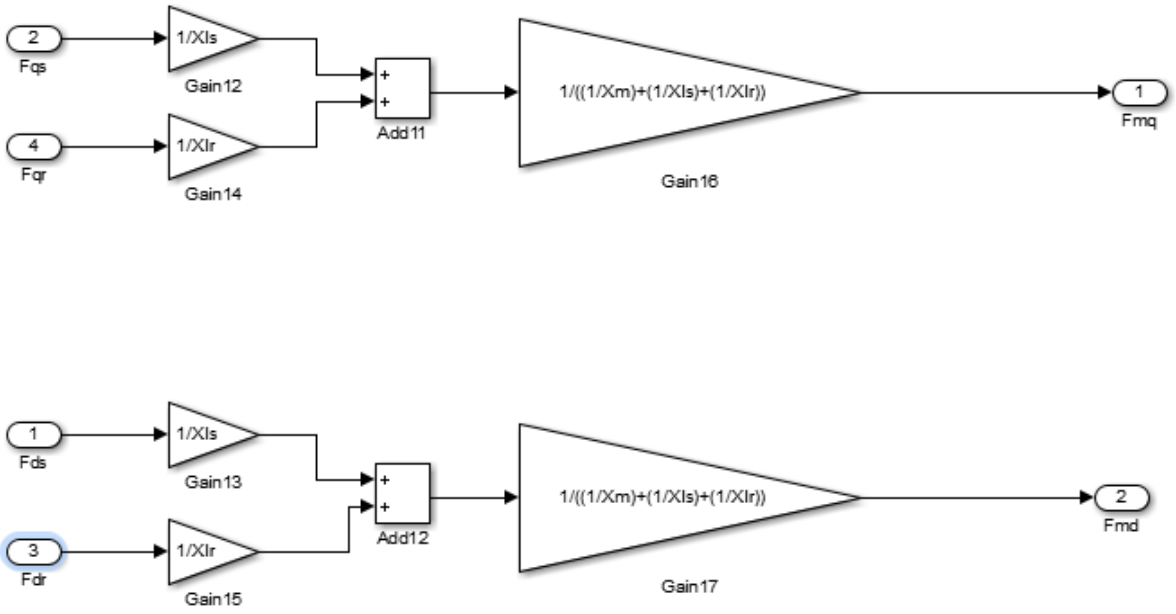

Figure 15: Implementation of flux linkage equations ψ_{mq} and ψ_{md}

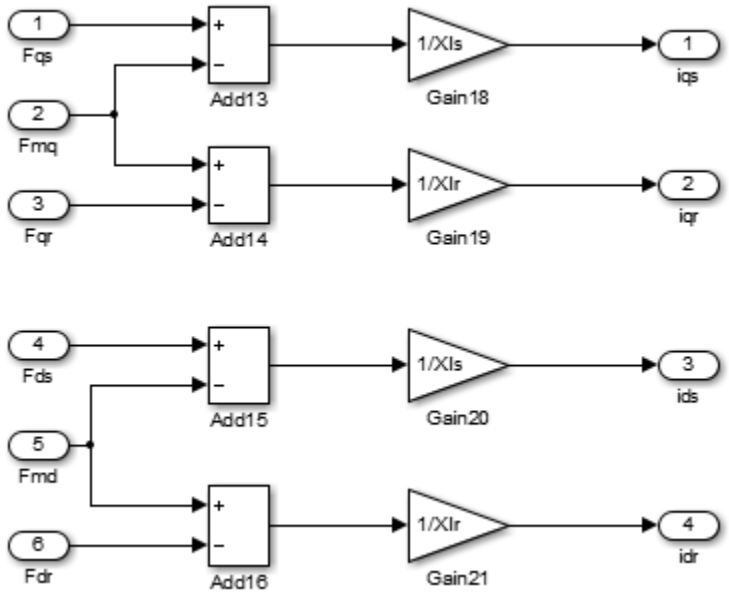

Figure 16: Implementation of current equations

Figure 17 represents the function blocks associated with the inverse parks transformation, the implementation of the torque equation and the equations associated with the rotor speed. Figures 18 and 19, show the implementation of the torque and speed equations respectively. While figure 20 shows the inverse park's transformation for the stator and rotor currents.

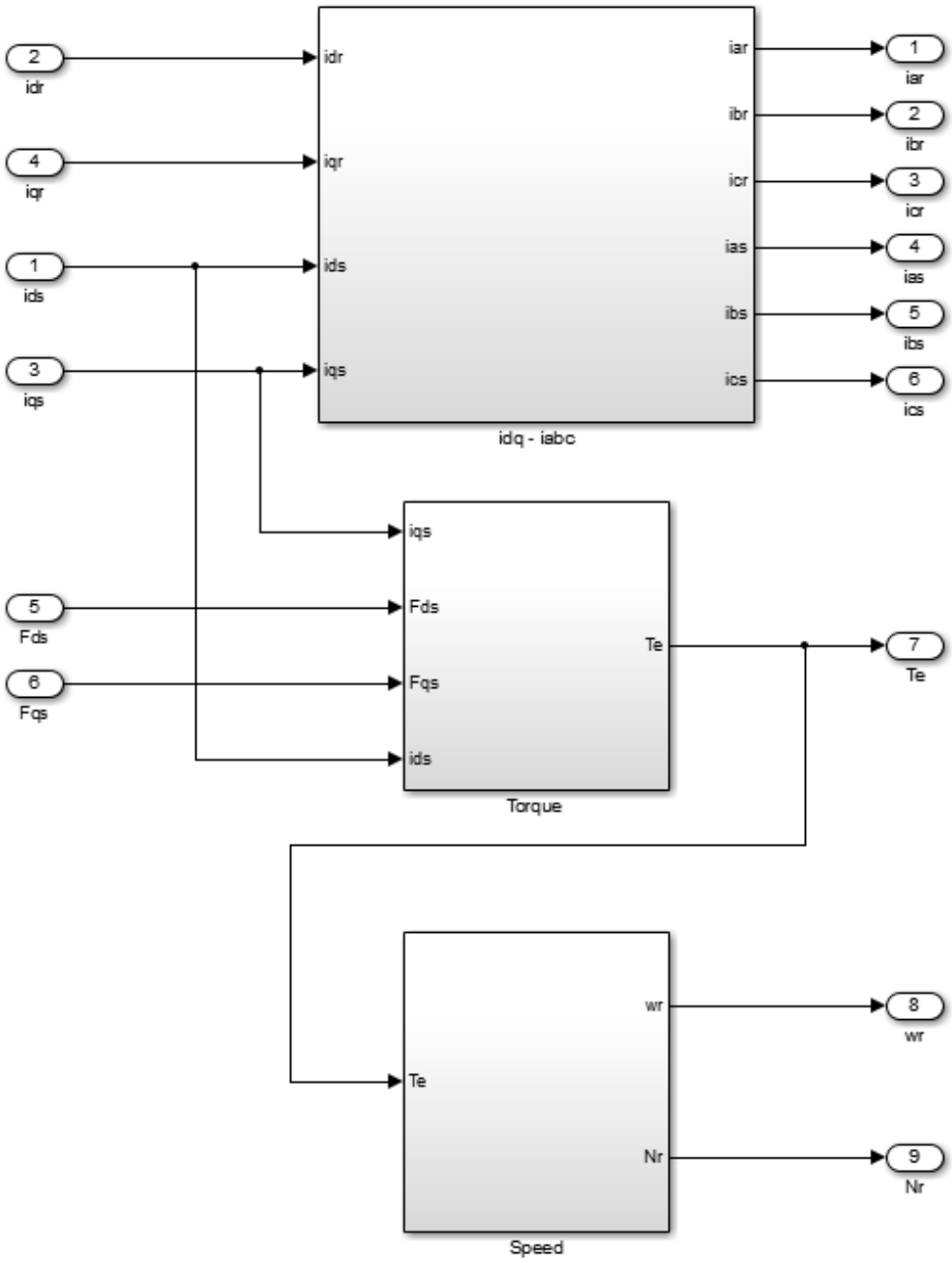

Figure 17: Function blocks for the inverse dq0 transformation for abc currents, torque equation and the speed equations

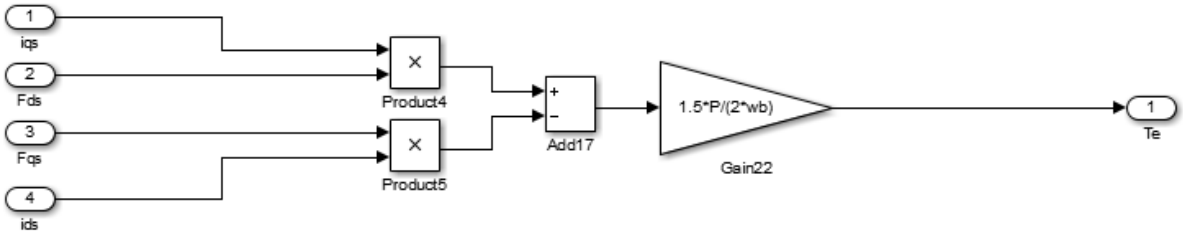

Figure 18: Implementation of the torque equation

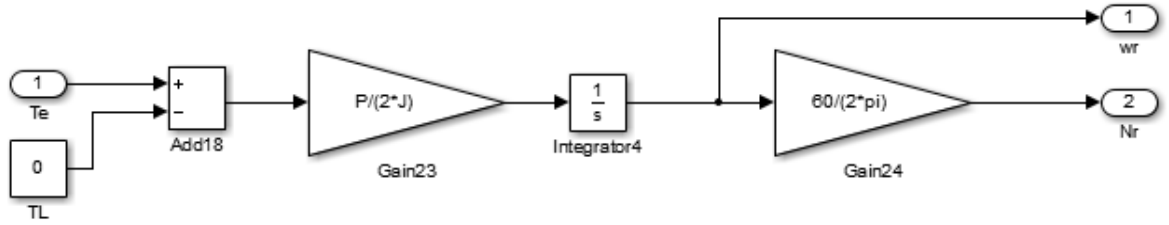

Figure 19: Angular speed equations

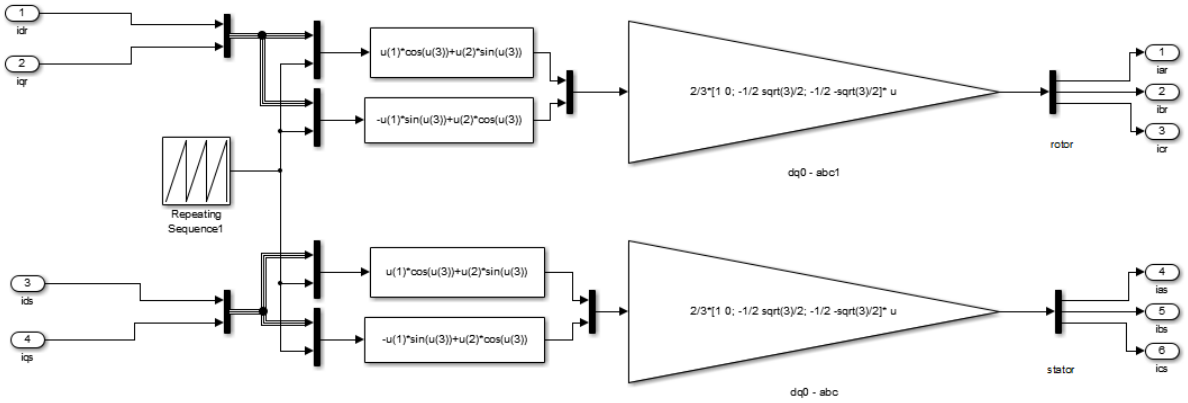

Figure 20: Inverse Park's transformation for currents

The final part was to create a .m file to define the variables in the equations used for the simulation. These included the line voltage, frequency, number of poles, moment of inertia, stator and rotor resistances and reactances, magnetising reactance and synchronous speed.

4.0 Results

4.1 DC test

Table 2: Results from DC test

	ϕ1-2	ϕ2-3	ϕ3-1	Average
V (volts dc)	49.40	49.20	49.40	49.33
I (amps dc)	1.02	1.02	1.02	1.02

4.2 No-load test

Table 3: Results from no-load test

	ϕ1	ϕ2	ϕ3	Average
V (volts)	418.80	418.63	419.10	418.84
I (amps)	0.9427	0.8930	0.9200	0.9186
f (Hz)				50
P (watts)				514.00

4.3 Blocked-rotor test

Table 4: Results from blocked-rotor test

	ϕ1	ϕ2	ϕ3	Average
V (volts)	68.40	69.20	68.70	68.77
I (amps)	1.0191	1.0260	1.0230	1.0227
f (Hz)	4.466	4.500	4.890	4.6187
P (watts)	135	138	137	136.67

4.4 Moment of inertia power test

4.4.1 No load

Table 5: Results from uncoupled motor power

ϕ1	ϕ2	ϕ3	Average

V (volts)	419.80	419.25	419.50	419.52
I (amps)	0.9115	0.8960	0.8840	0.8972
f (Hz)				50
P (watts)				492.00

4.4.2 Loaded

Table 6: Results from coupled motor power

	ϕ1	**ϕ2**	**ϕ3**	**Average**
V (volts)	419.60	419.00	419.25	419.28
I (amps)	0.9104	0.8980	0.8820	0.8968
f (Hz)				50
P (watts)				510.00

4.5 Equivalent Circuit Parameters

Calculating the equivalent circuit parameters from the method described in Method 1 yielded the following results:

- R_1 = 24.18 Ω
- R_2 = 0.97 Ω
- X_1 = 160.06 Ω
- X_2 = 160.06 Ω
- X_M = 166.19 Ω

The rotor resistance R_2 value derived from Method 2 resulted in a value of 19.3 Ω. However it was impossible to derive a value for the reactances as the calculated resistance was greater than the calculated impedance, as seen in Appendix 1.

```
% Motor Parameters

V = 240;          % phase voltage V
f = 50;           % Frequency Hz
```

```
P = 4;              % Number of Poles
J = 0.005;          % Inertia kgm^2
rr = 0.97;          % Rotor Resistance Ohms
rs = 24.18;         % Stator Resistance Ohms
Xlr = 160.06;       % Rotor Inductance Ohms
Xls = 160.06;       % Stator Inductance Ohms
Xm = 166.19;        % Magnetising Inductance Ohms
we = 157;           % Synchronous Speed rad/s
wb = 157;           % Base Speed rad/s
```

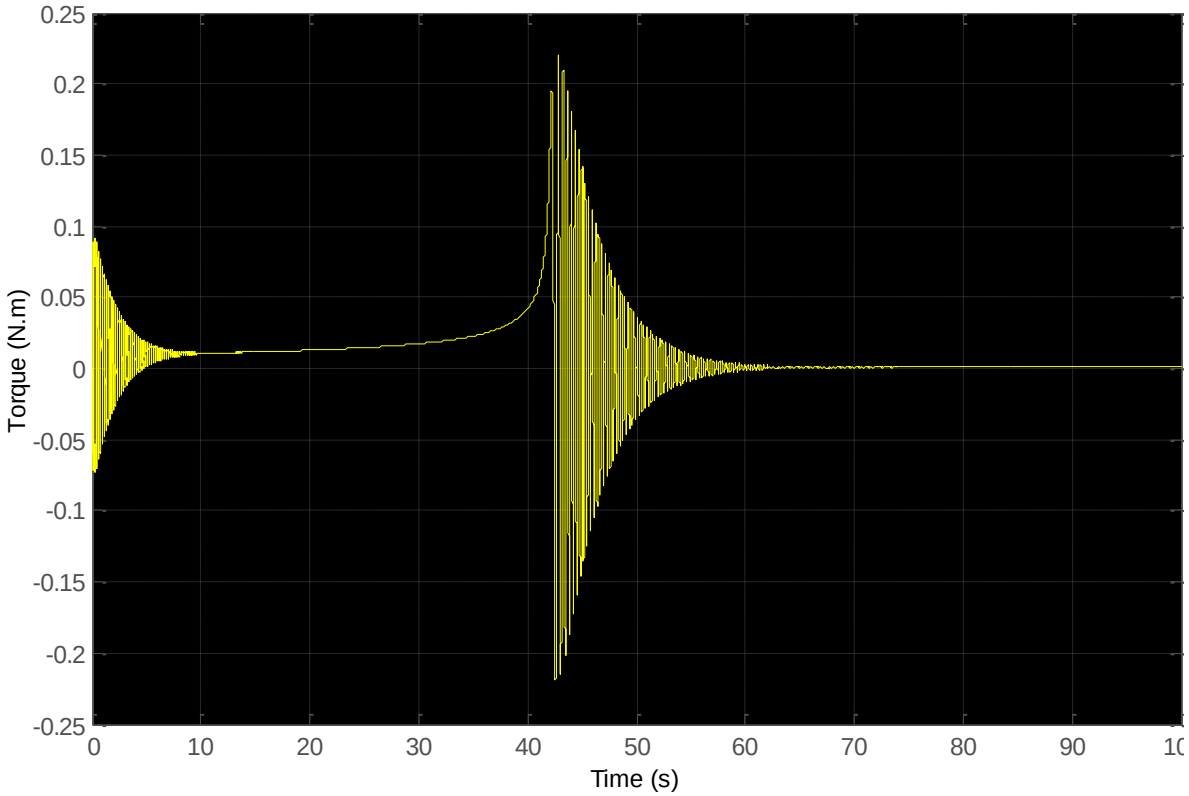

Figure 21: Torque-time characteristics for three-phase induction motor with parameters determined by method 1.

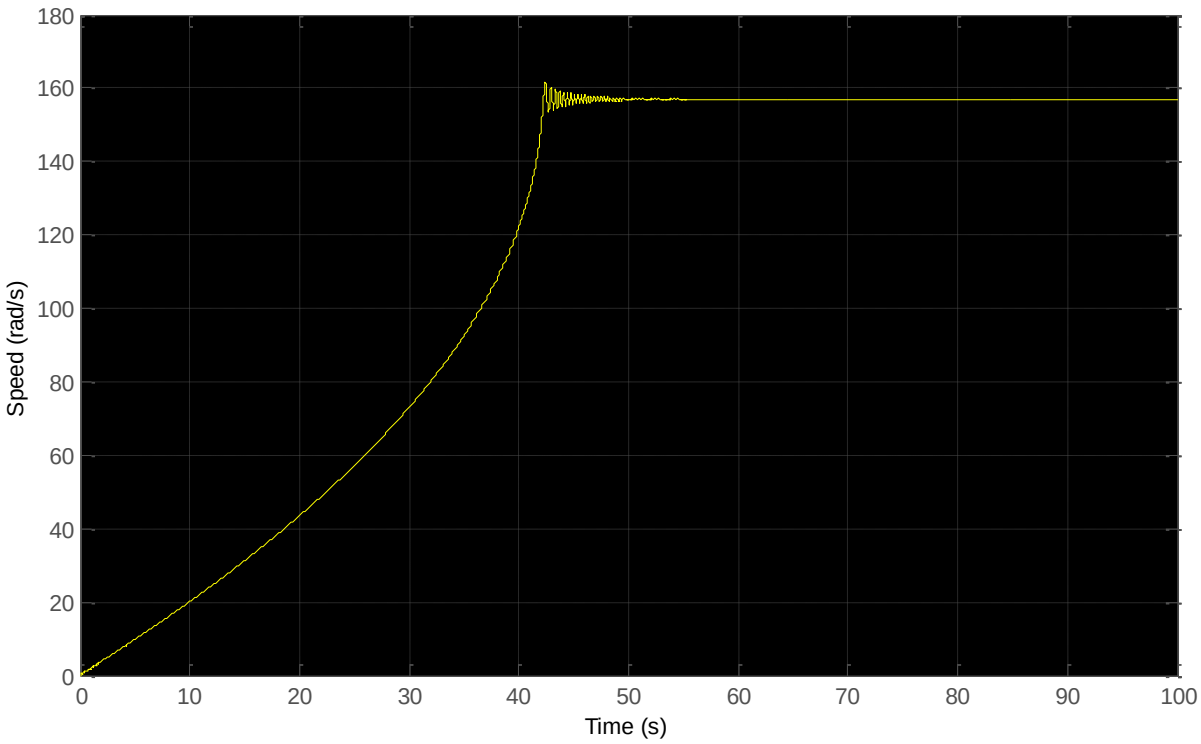

Figure 22: Speed-time characteristics from three-phase induction motor with parameters determined from method 1.

5 Discussion

5.1 DC Test

The results from the DC test proved to be the most accurate. A value of 25 ohms is what can be expected from a 0.37 kW three-phase induction motor. The results were also validated through the use of an external multimeter. The only discrepancy with this test is that a dc power supply does not reciprocate the 'skin' effect created by ac power.

5.2 No-Load Test

The no-load test had to be performed multiple times, as first the VSD did not reach the desired level of voltage or frequency for the motor to run at near synchronous speed. Also from the power tests used to determine the moment of inertia of the motor it was found that the results of active power from the power meter were wrong. This problem was eventually rectified through reversing two of the three phases entering the power meter. It was decided to perform this test with the motor connected directly to the mains supply. This would result in the required voltages and frequency being supplied to the motor, which would allow the motor to reach a speed as close as possible to its synchronous speed. This method is however not desirable, as the mains supply can be somewhat unpredictable, resulting in voltage or frequency fluctuations which could have detrimental effects on the motor.

5.3 Blocked-Rotor Test

The blocked-rotor test was also performed multiple times, because tests had to be repeated when the power meter was installed correctly. The use of a VSD was probably not the best motor drive to be used for this test, as the speed had to be increased until the line current value displayed on the power meter was equal to the rated current for the machine. This method proved undesirable as, for the protection of the motor, this test should be performed as fast as possible, and there was a considerable lag between the VSD and the results displayed on the power meter. This meant it was a tedious process trying to get the required speed that would result in the required current reading, meaning that the tests took much longer then they should have which could have possibly destroyed the motor through overheating the of stator windings.

5.4 Moment of Inertia Tests

The tests for the motor's moment of inertia proved to be inconclusive as it was impossible to obtain an accurate deceleration curve for the induction motor.

5.5 Loaded and Unloaded Power Tests

The results obtained from the original power test were deemed to be extremely inaccurate as the results for the active power measured were highly unlikely. The results indicated that the machine used less power when operated under load than when it was run unloaded from the same supply of power. These results indicated that the three-phase power meter was faulty. The power meter was replaced and the tests were again performed, which yielded the same obscure results. After much consideration and a thorough decipher of the user manual, it was deemed that the power meters settings were all correct. This issue was eventually rectified by reversing two of the three phases connected to the power meter. This yielded much more convincing results.

5.6 Deceleration Tests

The deceleration test proved to be impossible with the equipment provided. The motor came to a halt from a speed very close to synchronous speed in less than one and a half seconds. This did not allow time to obtain enough data points for an accurate plot of the motor's deceleration characteristics. In the time that it took for the motor to come to a complete rest the tachometer only displayed four to five readings; this included the maximum speed and zero speed. Therefore there were only two to three values which could be used to determine the curvature of the plot. Also, since this test took less than one and a half seconds the readings displayed on the tachometer were physically impossible to read in real time. This issue was rectified by filming the tachometer's response to the speed of the machine, and through the audio along with the visuals of the recordings it was possible to thoroughly analyse the tachometers readings. However, the results obtained by this method were also undesirable as there seemed to be a significant lag in the tachometer's recordings. This resulted in the deceleration curves of speed verses time to be almost linear. The results did not replicate normal deceleration curve, and therefore, it was decided that they would not be used to determine the motors moment of inertia.

5.7 Determination of Motors Equivalent Circuit Parameters

From the results obtained from the above circuit parameter tests, it was impossible to derive adequate circuit parameters. The method proposed in (Chapman, 2012)resulted in an R1 value of 0.7 ohms. This number is much too small to run an accurate simulation. The internal reactances of the motor were also much too high this resulted in the simulation taking far too long to reach steady state: it was observed during free acceleration that the motor would reach top speed in less than a second. Method 2 was then used to determine the equivalent circuit parameters, however this method proved impossible to derive a real value for reactances since R_{eq} was greater than Z_{eq}.

From being unable to perform the deceleration test with the proposed equipment, a value for the motor's moment of inertia could not be obtained. For this reason the value for the moment of inertia used in the simulation was left arbitrary. This enabled an appropriate moment of inertia value to be obtained through a trial and error method in running the simulation. The moment of inertia was varied throughout many simulations with the other parameters remaining constant until a simulation was performed which yielded results which somewhat paralleled the results expected for a three-phase induction motor. However with the derived circuit parameters this was often impossible. The simulation often paralleled the results expected from a much larger induction motor.

Due to the unrealistic results from the motor parameter tests, for the purpose of the simulation, the equivalent circuit parameters used were the value for the stator resistance, which proved to be accurate. And the value for the rotor resistance was used from METHOD 1. However the reactance values chosen to be simulated were derived also from METHOD 2, however it was decided not to transform these values to the equivalent values at the rated frequency. This enabled the values to be much more similar to I. Daut (2011).

6 Results

The following .m file was generated and the results were more typical of a low powered motor like the one attempted to be modelled in this paper.

```
% Motor Parameters

V = 240;          % phase voltage V
f = 50;           % Frequency Hz
P = 4;            % Number of Poles
J = 0.05;         % Inertia kgm^2
rr = 19.38;       % Rotor Resistance Ohms
rs = 24.18;       % Stator Resistance Ohms
Xlr = 25.61;      % Rotor Inductance Ohms
Xls = 25.61;      % Stator Inductance Ohms
Xm = 60.6;        % Magnetising Inductance Ohms
we = 157;         % Synchronous Speed rad/s
wb = 157;         % Base Speed rad/s
```

Figure 23 shows the three-phase input voltages being transformed into the dq0 reference frame. From the figure it can be seen that the three phases are 120 degrees apart, then after being transformed into the alpha beta reference frame there are only two phases separated by 90 degrees. Finally after the transformation into the synchronous reference frame, there are only two DC voltage quantities, where one is at the peak ($\sqrt{2} * 240$) and the other is at zero.

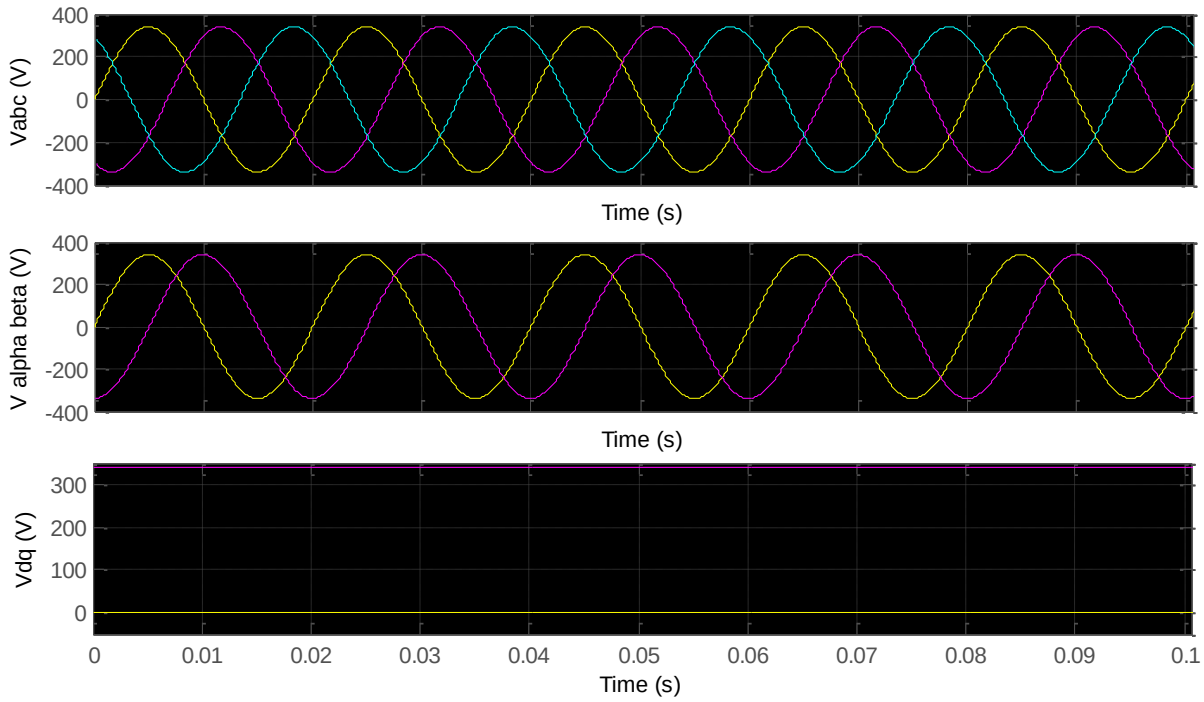

Figure 23: Three-phase input voltages in various reference frames

Figures 24 to 26 show the behaviour of the stator and rotor currents during the motors transient phase to synchronous speed. Figure 24 shows both the stator and rotor currents in the synchronous reference frame, while figures 25 and 26 show the behaviour of the rotor and stator currents respectively in the abc reference frame. From the figures it can be seen that the motor reaches synchronous speed in less than half a second, which is also expected for a small powered motor like the one being simulated. It can also be seen that during start-up, both the stator and rotor currents are significantly higher than during the synchronous speed phase, where the rotor currents go to zero. This is because a high current is needed to first move the motor and whilst at synchronous speed there is no induced voltage on the rotor, meaning no current will flow, which is why the rotor currents go to zero.

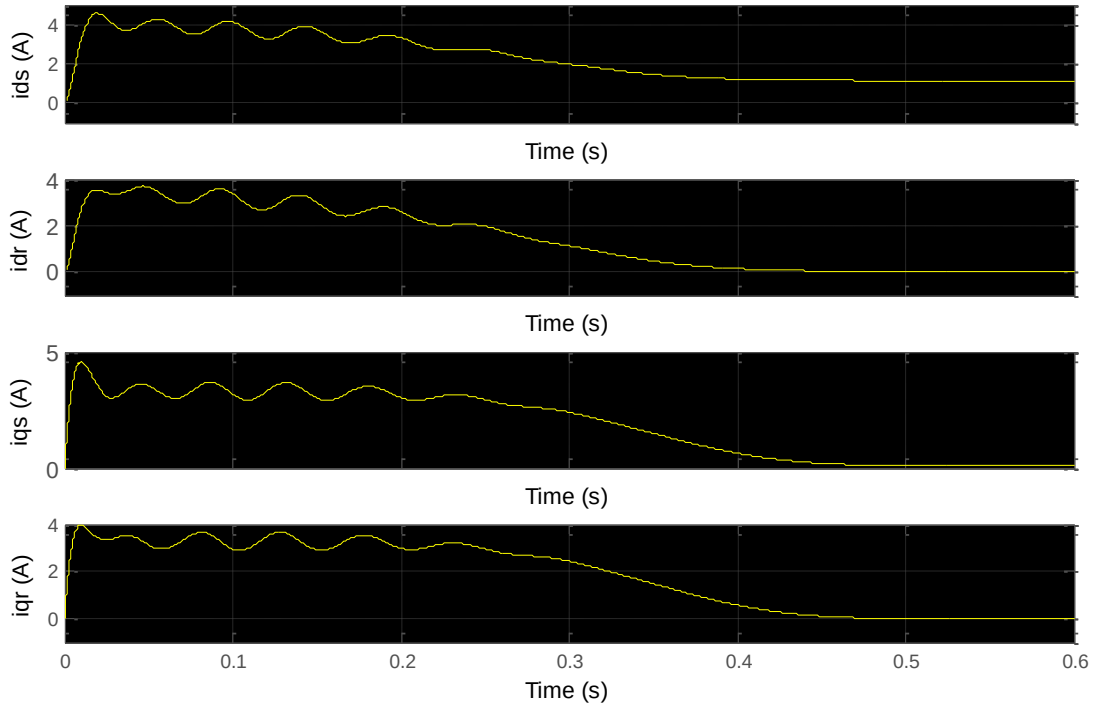

Figure 24: Stator and rotor currents in synchronous reference frame

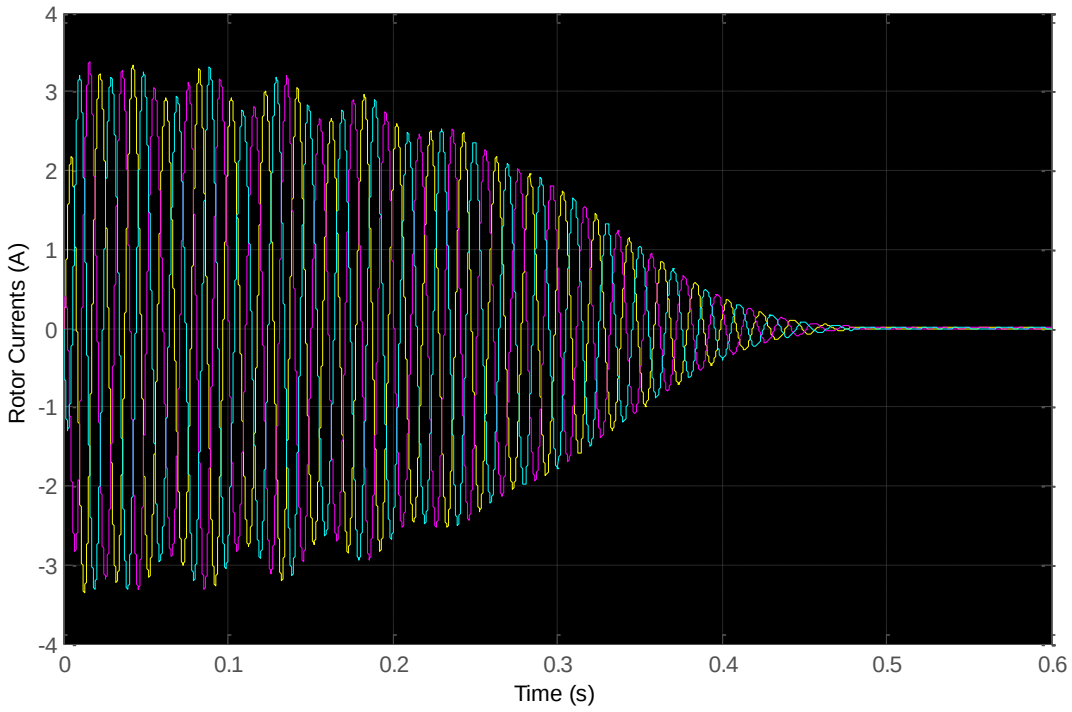

Figure 25: Rotor currents

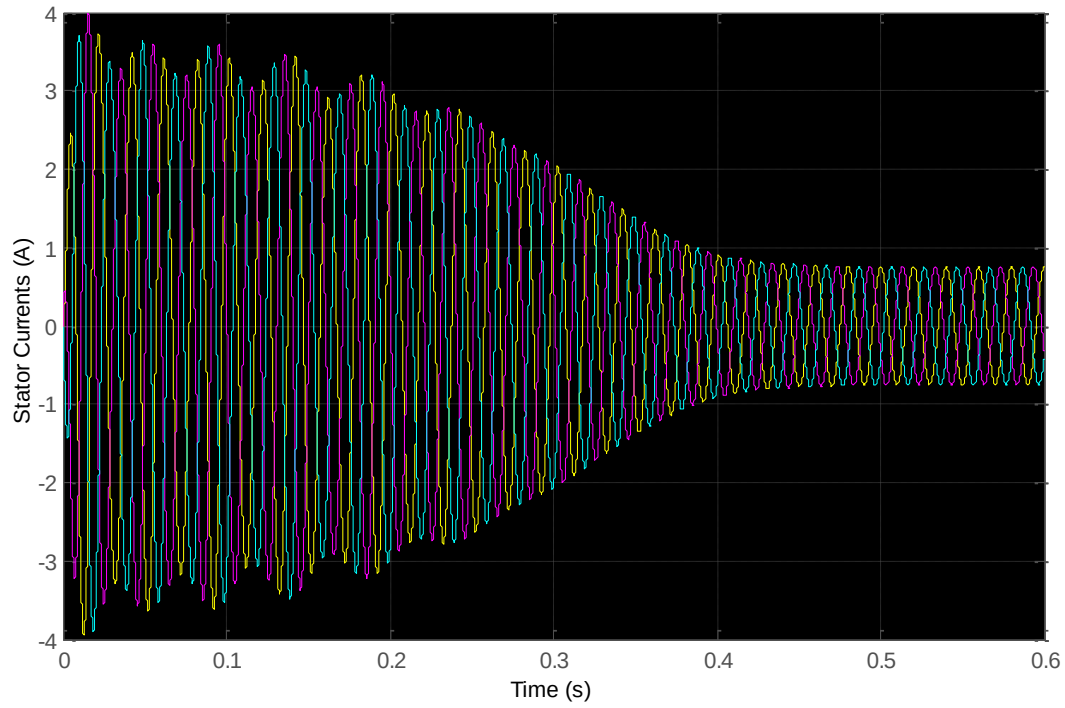

Figure 26: Stator currents

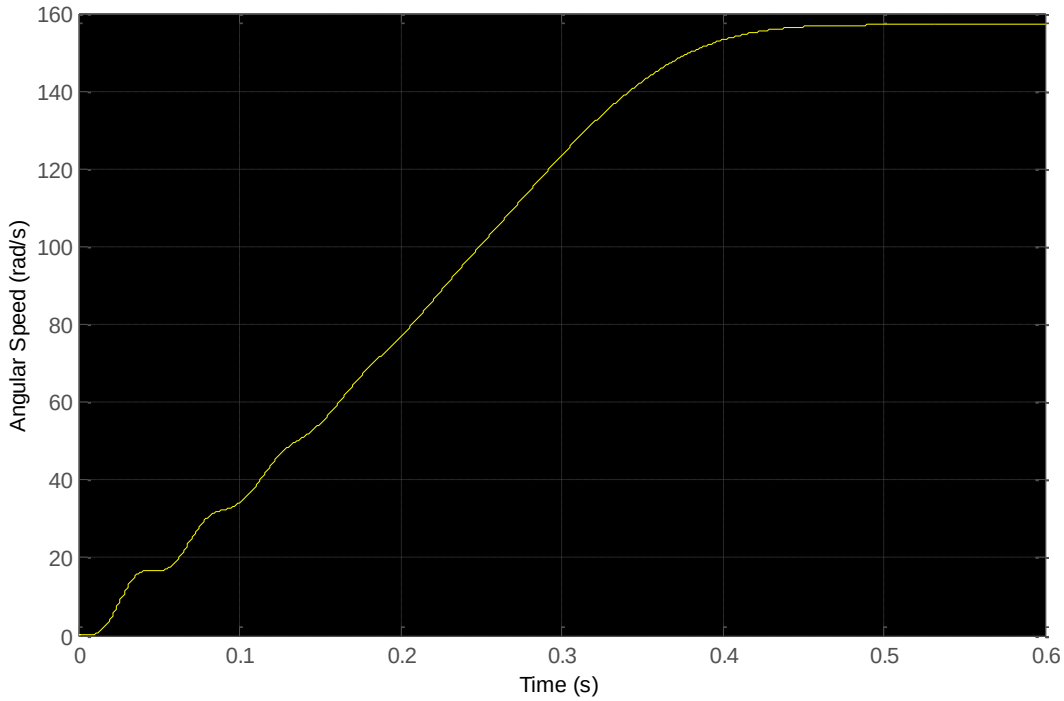

Figure 27: Angular velocity with respect to time

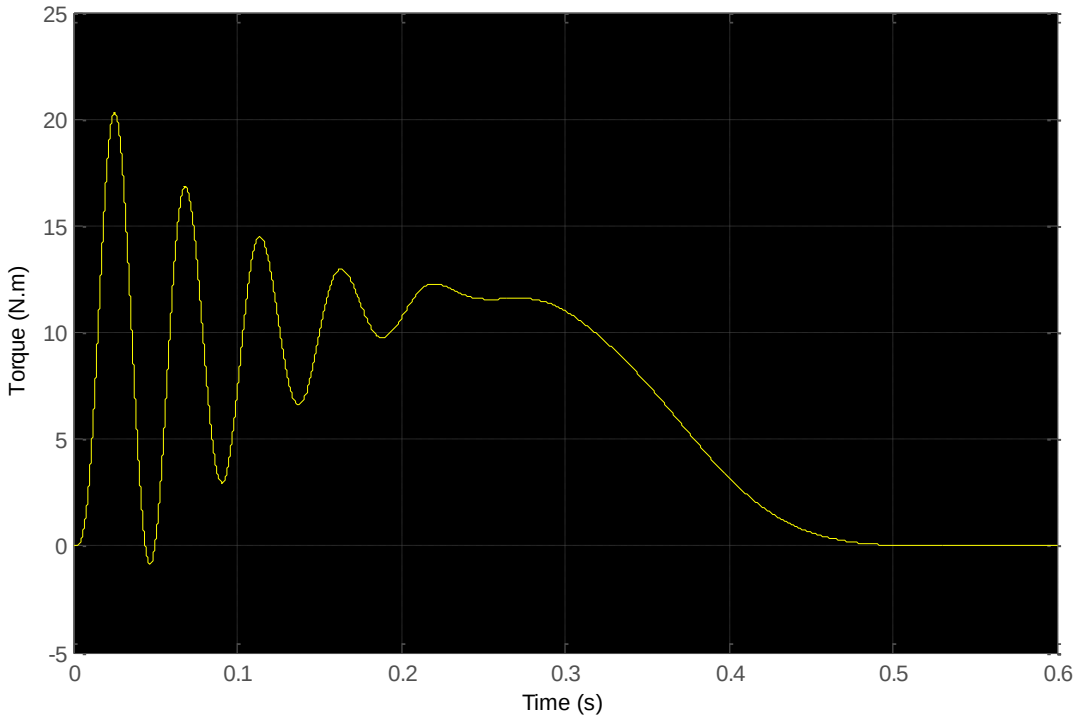

Figure 28: Induced torque with respect to time

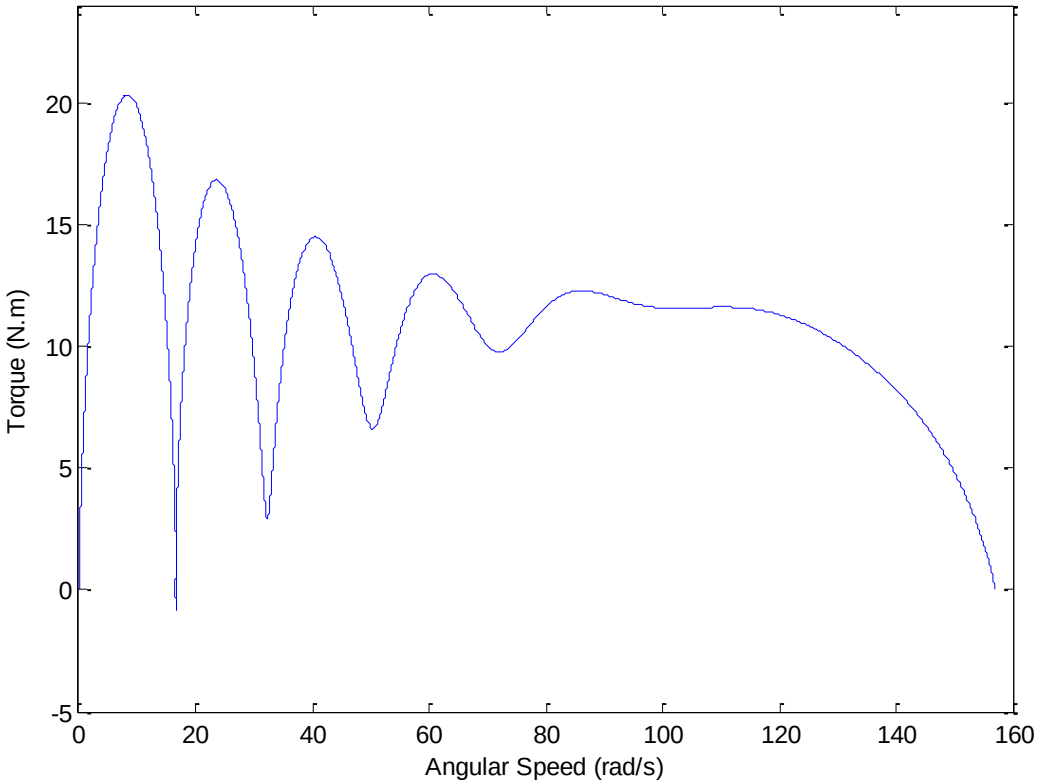

Figure 29: torque/Speed characteristics

From the obtained graphs the results were much more probable and were closer to the results shown in (P. C. Krause, 1965) and (Paul C. Krause, 2002). It can be seen that the motor reaches synchronous speed with full power applied in half a second, which is what can be expected. During start-up the stator and rotor currents are several times higher than the rated current which is what is expected and when synchronous speed is reached the rotor currents become zero. During acceleration the rotor velocity increases rapidly until it reaches synchronous speed, and does not overshoot as was the case earlier, which is what is expected for such a motor.

7 Conclusion

The three-phase induction motor is an extremely important motor in industry, and therefore it is important to understand its characteristics. Most of the characteristics for a three-phase induction motor cannot be simply measured; therefore it is highly advantageous to simulate such a motor. Even though obtaining the equivalent circuit parameters of the motor proved to be unsuccessful, this thesis shows that the MATLAB/Simulink computer program is a very helpful tool in performing such simulations. Motors of any size can be simulated using the proposed model if the equivalent circuit parameters are known.

It is also found that a change of reference frames greatly simplifies the analysis of three-phase induction machines by eliminating time varying inductances.

7.1 Future Work

For future work on this project, I would suggest re-performing the equivalent circuit parameter tests without bypassing the VSD. By bypassing the VSD the input voltage was too high yielding inaccurate results, which in turn resulted the equivalent circuit parameters that could not be determined. Also a better method needs to be implemented to determine the motors moment of inertia.

I would also suggest for future work that this project could involve: incorporating different drive systems into the simulation and comparing their performance; modelling and simulating motors of different sizes to understand the differences in their characteristics; and also simulating the motor in different reference frames to compare the differences.

Bibliography

A. L. Orille, G. M. (1999). A New Simulation of Symetrical Three Phase Induction Motor Under Transformation of Park. *Computers & Industrial Engineering*(37), 359-362.

al, L. G. (2010). The Modelling and Analysis of Asynchronous Motor Based on Matlab/Simulink. *International Conference on Computing, Control and Industrial Engineering*, (pp. 442-445).

Bilgin, H. A. (2012, June). Squirrel Cage of Induction Motors Simulation via Simulation. *International Journal of Modeling and Optimization, 2*(3), 324-327.

Chapman, S. J. (2012). Induction Motors. In S. J. Chapman, *Electric Machinery Fundamentals* (5th ed., pp. 307-396). New York: McGraw-Hill.

Ghanim, A. &. (2011). Dynamic Simulation of a Three-Phase Induction Motor Using Matlab Simulink. *Newfoundland Electrical and Computer Engineering Conference.* NECEC .

Hambley, A. R. (2008). AC Machines. In A. R. Hambley, *Electrical Engineering Principals and Applications* (4th ed., pp. 821-840). Pearson Education, Inc.

I. Daut, N. G. (2011). Modeling and Simulation of 0.5 HP Rotating Machine for the Investigation of Losses by using Copper as Rotor Bar Material. *Australian Journal of Basic and Applied Sciences*, 179-188.

(2009). The Three-Phase Squirrel-Cage Induction Motor. In J. Keljik, *Electricity 4 AC/DC Motors, Controls and Maintenance* (9th ed., pp. 105 - 125). Delmar, Cengage Learning.

Khorasani, M. H. (2008). N New Matlab Simulation of Induction Motor. *Australasian Universities Power Engineering Conference* (pp. 1-6). AUPEC'08.

Lee, K., Frank, S., Sen, P. K., Polese, L. G., Alahmad, M., & Waters, C. (2012). Estimation of induction motor equivalent circuit parameters from nameplate data. *2012 North American Power Symposium (NAPS)* (pp. 1-6). IEEE.

Ned Mohan, T. M. (2003). Induction Motor Drives. In T. M. Ned Mohan, *Power Electronics Converters, Applications and Design* (3rd ed., pp. 399-404). John Wiley & Sons.

P. C. Krause, C. H. (1965, November). Simulation of Symetrical Induction Machinery. *IEEE Transactions of Power Apparatus and Systems*(11), 1038-1053.

Park, R. H. (1929). Two-Reaction Theory of Synchronous Machines. *Transactions of the American Institute of Electrical Engineers, 48*(3), 716-727.

Paul C. Krause, O. W. (2002). Symetrical Induction Machines. In O. W. Paul C. Krause, *Analysis of Electric Machinery and Drive Systems* (2nd ed., pp. 141-190). John Wiley & Sons.

Puri, D. (n.d.). *Torque Equation of Three Phase Induction Motor*. Retrieved September 14, 2013, from Electrical Engineering: online electrical engineering study site: http://www.electrical4u.com/torque-equation-of-three-phase-induction-motor/

R. J. Lee, P. P. (1984/85). D, Q Reference Frames for the Simulation of Induction Motors. *Electric Power Systems Research, 8*, 15 - 26.

Sandhu, V. P. (2009, October). Transient Analysis of Three-Phase Induction Machine using Different Reference Frames. *ARPN Journal of Engineering and Applied Sciences, 4*(8), 31-38.

Shah, H. V. (2012). A Modular Simulink Implementation of Induction Machine Model & Performance in Different Reference Frames. *IEEE-International Conference On Advances In Engineering, Science And Managment* (pp. 203-206). IEEE.

Shakuntla Boora, S. K. (2013, August). Dynamic D-Q axis Modeling of Three-Phase Asynchronous Machine Using MATLAB. *International Journal of Advanced Research in Electrical, Electronics and Instrumentation Engineering, 2*(8), 3942-3951.

Sifat Shah, A. R. (2012, May). Direct Quadrature (D-Q) Modeling of a 3-Phase Induction Motor Using MATLAB/Simulink. *Canadian Journal on Electrical and Electronics Engineering, 3*(5), 237-243.

The Institute of Electrical and Electronic Engineers, Inc. (1996). IEEE Standard Test Procedure for Polyphase Induction Motors and Generators. *IEEE Std 112-1996*. The Institute of Electrical and Electronic Engineers, Inc.

Tolbert, B. O. (2003). Simulink Implementation of Induction Machine Model - A Modular Approach. 728-734.

Wadhwani, M. K. (n.d.). Transient Analysis of Three Phase Squirrel Cage Induction Machine using MATLAB. *International Journal of Engineering Research and Applications, 1*(3), 918-922.

Appendix 1

Three-phase induction motor equivalent circuit parameter tests

DC Test

DC Test

	ϕ1-2	**ϕ2-3**	**ϕ3-1**	**Average**
V (volts dc)	49.40	49.20	49.40	49.33
I (amps dc)	1.02	1.02	1.02	1.02

No-Load Test

The no-load test was performed by removing the VSD and connecting the power meter and the motor directly to the mains in order to achieve a phase voltage of approximately 240 volts and a frequency of 50 Hz.

V = 418.77 Volts $V = \frac{418.77}{\sqrt{3}} = 241.77\ Volts$

I = 0.8932 Amps

S = 1.1524 kVA

Q = 1.0902 kVAr

F = 51.50 Hz

$$P = \sqrt{S^2 - Q^2} = \sqrt{1.1524\ k^2 - 1.0902\ k^2} = 0.3735\ kW = 373.5\ W$$

No Load

	ϕ1	**ϕ2**	**ϕ3**	**Average**
V (volts)	418.80	418.63	419.10	418.84
I (amps)	0.9427	0.8930	0.9200	0.9186

Frequency = 50 Hz

Power = 514 W

Blocked-Rotor Test

	ϕ1	ϕ2	ϕ3	Average
V (volts)	67.5	67.73	67.24	67.49
I (amps)	1.0200	1.0260	1.0204	1.0221
S (kVA)	0.2058	0.2083	0.2055	0.2065
Q (kVAr)	0.1505	0.1524	0.1512	0.1514
f (Hz)	4.3950	4.3960	4.3975	4.3962

$$P = \sqrt{S^2 - Q^2} = \sqrt{0.2065\ k^2 - 0.1514\ k^2} = 0.1404\ kW = 140.4\ W$$

Blocked Rotor

	ϕ1	**ϕ2**	**ϕ3**	**Average**
V (volts)	68.40	69.20	68.70	68.77
I (amps)	1.0191	1.0260	1.0230	1.0227
f (Hz)	4.466	4.500	4.890	4.6187
P (watts)	135	138	137	136.67

Calculating the Motor Parameters

METHOD 1

$$P_{BR,fm} = \frac{136.67\ W}{3} = 45.56\ W$$

$$V_{BR,fm} = \frac{68.77\ V}{\sqrt{3}} = 39.70\ V$$

$$I_{BR,fm} = 1.0227\ A$$

$$P_{NL} = \frac{514\ W}{3} = 171.33\ W$$

$$V_{NL} = \frac{418.84\ V}{\sqrt{3}} = 241.82\ V$$

$$I_{NL} = 0.9186\ A$$

$$|Z_{NL}| = \frac{V_{NL}}{I_{NL}} = \frac{240.82\ V}{0.9186\ A} = 263.25\ \Omega = X_1 + X_M$$

$$Z_{BR,fm} = \frac{V_{BR,fm}}{I_{BR,fm}} = \frac{39.7\ V}{1.0227\ A} = 38.82\ \Omega$$

$$\theta = cos^{-1}\left(\frac{P_{in}}{\sqrt{3}V_{BR}I_{BR}}\right) = cos^{-1}\frac{45.56}{70.33} = cos^{-1}0.6478 = 49.62°$$

$$R_{BR} = |Z_{BR}|cos\theta = 38.82 * cos49.62° = 25.15\ \Omega$$

$$R_2 = R_{BR} - R_1 = 25.15 - 24.18 = 0.97\ \Omega$$

$$X'_{BR\ fm} = |Z_{BR}|sin\theta = 38.82 * sin\ 49.62 = 29.57\ \Omega$$

$$X_{BR} = \left(\frac{f_{rated}}{f_{measured}}\right)X_{BR.fm} = \left(\frac{50\ Hz}{4.6187\ Hz}\right)29.57\ \Omega = 320.11\ \Omega$$

$$X_1 = X_2 = \frac{X_{BR}}{2} = \frac{320.11\ \Omega}{2} = 160.06\ \Omega$$

$$X_M = Z_{NL} - X_1 = 326.25\ \Omega - 160.06\ \Omega = 166.19\ \Omega$$

METHOD 2

The first step was to transform the test data to the corresponding phase values for a wye-connected motor.

$$P_{BR,fm} = \frac{136.67\ W}{3} = 45.56\ W$$

$$V_{BR,fm} = \frac{68.77\ V}{\sqrt{3}} = 39.70\ V$$

$$I_{BR,fm} = 1.0227\ A$$

$$P_{NL} = \frac{514\ W}{3} = 171.33\ W$$

$$V_{NL} = \frac{418.84\ V}{\sqrt{3}} = 241.82\ V$$

$$I_{NL} = 0.9186\ A$$

Where the subscripts; *BR, fm* and *NL* refer to the measured values from the blocked-rotor tests and the no-load tests respectively.

The next step is to determine the stator resistance, R_1, where:

$$R_1 = \frac{R_{DC}}{2}$$

R_{DC} is calculated from the data from the DC test using ohms law:

$$R_{DC} = \frac{V_{DC}}{I_{DC}} = \frac{49.33\ V}{1.02\ A} = 48.36\ \Omega$$

Since the stator is wye-connected, R_{DC} is the resistance through two phases, therefore:

$$R_1 = \frac{R_{DC}}{2} = \frac{48.36\ \Omega}{2} = 24.18\ \Omega$$

The next step is to determine the rotor resistance R_2.

$$Z_{BR,fm} = \frac{V_{BR,fm}}{I_{BR,fm}} = \frac{39.7\ V}{1.0227\ A} = 38.82\ \Omega$$

$$R_{BR,fm} = \frac{P_{BR,fm}}{I_{BR,fm}^2} = \frac{45.56\ W}{1.0227^2\ A} = 43.56\ \Omega$$

$$R_2 = R_{BR,fm} - R_1 = 43.56\ \Omega - 24.18\ \Omega = 19.38\ \Omega$$

Again using the blocked-rotor measurements to calculate the stator and rotor inductances:

$$X_{BR.fm} = \sqrt{Z_{BR,fm}^2 - R_{BR,fm}^2} = \sqrt{38.82^2 - 43.56^2} = 19.76i\ \Omega$$

As it can be seen there is no real solution for the above equation

Now calculating X_{BR} at the rated frequency, 50 Hz:

$$X_{BR} = \left(\frac{f_{rated}}{f_{measured}}\right) X_{BR.fm} = \left(\frac{50\ Hz}{4.6187\ Hz}\right) 19.76\ \Omega = 213.91\ \Omega$$

For a design A machine:

$$X_1 = X_2 = \frac{X_{BR}}{2} = \frac{213.91\ \Omega}{2} = 106.96\ \Omega$$

The next step is to use the data from the no-load measurements to determine the magnetising inductance, X_M.

$$S_{NL} = V_{NL} I_{NL} = 241.82\ V * 0.9186\ A = 222.14\ VA$$

$$S_{NL} = \sqrt{P_{NL}^2 + Q_{NL}^2}$$

$$Q_{NL} = \sqrt{S_{NL}^2 - P_{NL}^2} = \sqrt{222.14^2 - 171.33^2} = 141.39\ VAr$$

$$Q_{NL} = I_{NL}^2 X_{NL}$$

$$X_{NL} = \frac{Q_{NL}}{I_{NL}^2} = \frac{141.39\ VAr}{0.9186^{\,2}\ A} = 167.56\ \Omega$$

So rearranging the equation:

$$X_{NL} = X_1 + X_M$$

And substituting in X_1:

$$X_M = X_{NL} - X_1 = 167.56\ \Omega - 106.96\ \Omega = 60.6\ \Omega$$

Appendix 2

Appendix 2 can be found on the attached CD ROM.